Report No. F-69-5



# THEORETICAL INVESTIGATION OF CROSSFLOW EFFECTS ON COMPRESSIBLE TURBULENT BOUNDARY LAYER OVER BODIES OF REVOLUTION

by



Victor Zakkay

and

Wladimiro Calarese

Department of Aeronautics and Astronautics

Prepared for the

Office of University Affairs

National Aeronautics and Space Administration

under Grant

NGL-33-016-067

New York University
School of Engineering and Science
University Heights, New York, N.Y. 10453

December 1969

Report No. F-69-5

NEW YORK UNIVERSITY
New York, New York

# THEORETICAL INVESTIGATION OF CROSSFLOW EFFECTS ON COMPRESSIBLE TURBULENT BOUNDARY LAYER OVER BODIES OF REVOLUTION

by

Victor Zakkay
Professor

and

Wladimiro Calarese
Assistant Research Scientist

Department of Aeronautics and Astronautics

School of Engineering and Science

Prepared for The Office of University Affairs
National Aeronautics and Space Administration
under Research Grant NGL-33-016-067

December 1969

## ABSTRACT

An analysis for the compressible turbulent boundary layer undergoing both adverse pressure gradient and crossflow along a plane of symmetry is presented.

The purpose of this investigation is to provide a method for calculating boundary layers such as the ones that occur on the centerline of symmetry of an inlet.

The three dimensional compressible integral equations are written along the symmetry plane, and integrated numerically, and in addition the effect of crossflow and the behavior of the boundary layer is also studied.

Included in the report are comparisons with the sparse amount of experimental results available in the literature. While this part of the report describes the working equations for the analysis, a second part will follow whereby a more extensive experimental investigation will be presented in detail, and a final comparison with the experimental results will be performed.

## List of Symbols

| | |
|---|---|
| $a$ | Speed of sound |
| $A$ | Constant defined in Eq. II-16 |
| $B$ | Constant defined in Eq. II-16 |
| $C$ | Constant defined in Eq. III-3 |
| $C_f$ | Coefficient of friction |
| $D$ | Constant defined in Eq. II-16 |
| $h$ | Static enthalpy |
| $H$ | Stagnation enthalpy |
| $\bar{H}$ | Form factor $\frac{\delta^*}{\theta}$ |
| $H^*$ | $H-H_w$ |
| $H_e^*$ | $H_e-H_w$ |
| $k$ | Constant defined in Eq. III-2A |
| $\dot{m}$ | Mass flux |
| $M$ | Mach number |
| $N$ | Power law exponent |
| $p$ | Pressure |
| $\bar{p}$ | $p_e/(p_e)_{Mer.}$ |
| $Pr$ | Prandtl number |
| $r$ | Body radius |
| $Re$ | Reynolds number |
| $s$ | Direction of the inviscid streamline |

$s'$ Streamwise distance measured from beginning of flare

$s_1, x$ Projection of the inviscid streamline on the body surface

$T$ Temperature

$u$ Velocity in streamwise direction

$v$ Velocity normal to the surface of the body

$w$ Velocity in the peripheral direction

$y$ Direction normal to the surface of the body

$\alpha$ Angle of attack

$\gamma$ Specific heat ratio

$\delta^*$ Integral parameter for the displacement thickness

$\eta_c$ Cone semivertex angle

$\theta$ Integral parameter for the momentum thickness

$\mu$ Viscosity

$\nu$ Kinematic viscosity

$\rho$ Density

$\tau_o$ Shear stress at the wall

$\varphi$ Orthogonal trajectory of the projection of the inviscid streamline on the body surface, peripheral angle

$\Phi$ Integral parameter for the energy thickness

Subscripts

B.F. Beginning of flare

Cyl. Cylinder

e External conditions

i,1 Initial conditions

L Edge of laminar sublayer

Mer Meridian

o Stagnation conditions

v Viscous

w Wall conditions

z Zero angle of attack

$\infty$ Free stream conditions

$\delta$ Based on boundary layer thickness

$\theta$ Based on momentum thickness

Superscripts

(') Reference quantities

(") Inches

## INTRODUCTION

Recently there has been a large amount of work being performed on air breathing propulsion systems, especially for determining flow fields over the various configurations.

The boundary layer on axially symmetric configurations has been studied by several investigators (Refs. 2,7) however, very little work has been performed for three dimensional configurations.

The inlet part of the engine plays an important role in the determination of the overall performance of the propulsion system. Of direct interest is its boundary layer characteristics which place an upper limit on the maximum pressure rise without separating the flow within the inlet. Methods of avoiding this separation may be achieved by boundary layer bleed or by designing a three dimensional inlet. The relative advantages of three dimensional inlet designs are already known, and it is for this reason that this detailed study of the behavior of the boundary layer under both adverse pressure gradient as well as favorable crossflow is undertaken.

In spite of the fact that an adverse crossflow which results from the wall of the inlet presents the upper criteria for separation, and is the more difficult to analyze, this research will be concerned with the favorable crossflow condition, and its effect on the turbulent boundary layer behavior.

For the analysis, the momemtum integral equations in the axial and peripheral direction, in addition to the energy equations, are used. The axial momentum equation becomes independent of the peripheral one along the symmetry plane, and therefore simplifies the analysis. In addition to the adverse

pressure gradient produced by the inlet surface, it is well known that there are present significant pressure gradients normal to the wall, which tend to enhance the probability of boundary layer separations.

Instead of treating the boundary layer under all these conditions, the normal gradients or the effect of $\partial p/\partial y$ on the behavior of the boundary layer is treated in the same manner as in Refs. 7, 10, and 17.

This procedure consists of determining the boundary layer characteristics such as ($\delta, \delta^*$ and $\theta$) under $\partial p/\partial y = 0$, and adding to this the contributions due to the inviscid rotational flowfield. This method was found to be good for the axially symmetric case, and will be proved adequate subsequently in part 2 of this paper.

In addition, the analyses are finally compared with the experimental results of Ref. 6 for a cone at an angle of attack, and with the theories of Refs. 11 and 12, which refer to the two dimensional case.

I. Integral Equations:

An orthogonal system of geodesic coordinates $(x,\varphi,y)$ was chosen.(Fig. 1) The x curves ($\varphi$=const) are the projection of the inviscid streamline on the surface of the body and the $\varphi$ curves (x=const.) are the orthogonal trajectories of the projection. The surface of the body is located at y=0. A linear element $ds^2$ is given by (Fig. 1)

$$ds^2=dx^2+ r^2\ d\varphi^2+dy^2 \qquad \text{(Fig. 2)}$$

In this coordinate system, assuming zero normal pressure gradient, the steady boundary layer momentum equations are:

$$\rho\left(u \frac{\partial u}{\partial x} + v \frac{\partial u}{\partial y} + \frac{w}{r} \frac{\partial u}{\partial \varphi} - \frac{1}{r} \frac{dr}{dx} w^2\right) = - \frac{\partial p}{\partial x} + \frac{\partial}{\partial y} \left(\mu \frac{\partial u}{\partial y}\right) \qquad \text{(I-1)}$$

$$\rho\left(u \frac{\partial w}{\partial x} + \frac{w}{r} \frac{\partial w}{\partial \varphi} + v \frac{\partial w}{\partial y} + \frac{1}{r} \frac{dr}{dx} uw\right) = - \frac{1}{r} \frac{\partial p}{\partial \varphi} + \frac{\partial}{\partial y} \left(\mu \frac{\partial w}{\partial y}\right) \qquad \text{(I-2)}$$

$$0 = \frac{\partial p}{\partial y} \qquad \text{(I-3)}$$

Energy equation

$$\rho \left(u \frac{\partial H}{\partial x} + \frac{w}{r} \frac{\partial H}{\partial \varphi} + v \frac{\partial H}{\partial y}\right) = \frac{\partial}{\partial y} \left\{ \mu \left(\frac{\partial H}{\partial y} + \frac{1-Pr}{Pr} \frac{\partial h}{\partial y}\right) \right\} \qquad \text{(I-4)}$$

Continuity equation

$$\frac{\partial}{\partial x} (\rho ru) + \frac{\partial}{\partial \varphi} (\rho w) + \frac{\partial}{\partial y} (\rho rv) = 0 \qquad \text{(I-5)}$$

At y=0, u=v=w=o, and at $y=\delta$, $u=u_e$, and $v_e=w_e=0$, therefore the boundary conditions for Eq. (I-1) are:

$$\rho_e u_e \frac{du_e}{dx} = - \frac{\partial p}{\partial x} \qquad \text{(I-6)}$$

$$\left[\frac{\partial}{\partial y} \left(\mu \frac{\partial u}{\partial y}\right)\right]_{y=0} = \frac{\partial p}{\partial x} \qquad \text{(I-7)}$$

In order to derive the integral form of Eq. (I-1) we make use of the continuity eq. (I-5), from which

$$v = - \frac{1}{\rho r} \int_o^y \left[ \frac{\partial}{\partial x}(\rho r u) + \frac{\partial}{\partial \varphi} (\rho w) \right] dy \qquad \text{(I-8)}$$

Substituting for v in Eq. (I-1), integrating term by term from zero to $\delta$, and using the boundary conditions, we obtain [see Appendix 1]

$$\frac{d\theta}{dx} = - \left[ (\bar{H}+2) \frac{1}{u_e} \frac{du_e}{dx} + \frac{1}{\rho_e} \frac{d\rho_e}{dx} + \frac{1}{r} \frac{dr}{dx} \right] \theta$$

$$- \frac{1}{r u_e} \left( \frac{\partial w}{\partial \varphi} \right)_{Mer.} \int_o^\delta \frac{\rho}{\rho_e} \left( 1 - \frac{u}{u_e} \right) dy + {}^{C_f}/_2 \qquad \text{(I-9)}$$

where

$$\theta = \int_o^\delta \frac{\rho u}{\rho_e u_e} \left( 1 - \frac{u}{u_e} \right) dy \qquad \text{(I-10)}$$

$$\delta^* = \int_o^\delta \left( 1 - \frac{\rho u}{\rho_e u_e} \right) dy \qquad \text{(I-11)}$$

$$\bar{H} = \frac{\delta^*}{\theta} \qquad \text{(I-12)}$$

The energy equation (I-4), for unity Prandtl number, is

$$\rho \left( u \frac{\partial H}{\partial x} + \frac{w}{r} \frac{\partial H}{\partial \varphi} + v \frac{\partial H}{\partial y} \right) = \frac{\partial}{\partial y} \left( \mu \frac{\partial H}{\partial y} \right) \qquad \text{(I-13)}$$

using continuity (Eq. I-5),

$$\rho \left\{ u \frac{\partial H}{\partial x} + \frac{w}{r} \frac{\partial H}{\partial \varphi} - \left[ \frac{1}{\rho r} \int_o^y \left( \frac{\partial}{\partial x} (\rho r u) + \frac{\partial}{\partial \varphi} (\rho w) \right) dy \right] \frac{\partial H}{\partial y} \right\} =$$

$$= \frac{\partial}{\partial y} \left( \mu \frac{\partial H}{\partial y} \right) \qquad \text{(I-14)}$$

Integrating term by term throughout the boundary layer, we obtain

[ see Appendix 2 ]

$$\frac{d\Phi}{dx} = -\left[\frac{1}{u_e}\frac{du_e}{dx} + \frac{1}{\rho_e}\frac{d\rho_e}{dx} + \frac{1}{r}\frac{dr}{dx}\right]\Phi - \frac{1}{ru_e}\left(\frac{\partial w}{\partial \varphi}\right)_{Mer.}\int_o^\delta \frac{\rho}{\rho_e}\left(1-\frac{H^*}{H_e^*}\right)dy$$

$$= \frac{q_w}{\rho_e u_e H_e^*} \qquad (I\text{-}15)$$

II. Evaluation of the Cross-flow Parameter

The momentum integral equation in the streamwise direction and the energy integral equation differ from the standard axisymmetric ones by the term where $\left(\frac{\partial w}{\partial \varphi}\right)_{Mer.}$ appears, due to the presence of crossflow. $\left(\frac{\partial w}{\partial \varphi}\right)_{Mer.}$ depends on the inviscid pressure distribution on the body and, therefore, the inviscid momentum equation in the peripheral direction is used to evaluate it.

Equation I-2 becomes

$$u\frac{\partial w}{\partial x} + \frac{w}{r}\frac{\partial w}{\partial \varphi} + \frac{1}{r}\frac{dr}{dx}uw = -\frac{1}{\rho r}\frac{\partial p}{\partial \varphi} \qquad (II\text{-}1)$$

If the pressure distribution over the body under consideration is known from theory or experiment, we can find a relationship between $\frac{\partial w}{\partial \varphi}$ and $\frac{\partial p}{\partial \varphi}$.

Differentiating equation II-1 with respect to $\varphi$ we get

$$\frac{\partial w}{\partial \varphi}\frac{\partial w}{\partial x} + u\frac{\partial^2 w}{\partial \varphi \partial x} + \frac{1}{r}\left(\frac{\partial w}{\partial \varphi}\right)^2 + \frac{w}{r}\frac{\partial^2 w}{\partial \varphi^2} + \frac{1}{r}\frac{dr}{dx}u\frac{\partial w}{\partial \varphi} +$$

$$+ \frac{1}{r}\frac{dr}{dx}w\frac{\partial u}{\partial \varphi} = -\frac{1}{\rho r}\frac{\partial^2 p}{\partial \varphi^2} + \frac{1}{\rho^2 r}\frac{\partial p}{\partial \varphi}\frac{\partial \rho}{\partial \varphi} \qquad (II\text{-}2)$$

Evaluating eq. II-2 at the meridian plane, i.e. where $w = \frac{\partial u}{\partial \varphi} = \frac{\partial \rho}{\partial \varphi} = 0$, we get

$$u\frac{\partial^2 w}{\partial \varphi \partial x} + \frac{1}{r}\left(\frac{\partial w}{\partial \varphi}\right)^2 + \frac{1}{r}\frac{dr}{dx}u\frac{\partial w}{\partial \varphi} + \frac{1}{\rho r}\frac{\partial^2 p}{\partial \varphi^2} = 0 \qquad (II\text{-}3)$$

Defining $\frac{w}{u_e} = w^*$ and noting that $u \equiv u_e$ in the inviscid momentum equation under consideration and $p \equiv p_e$ if we assume zero normal pressure gradient, Eq. II-3 becomes

$$\frac{\partial}{\partial x}\left(\frac{\partial w^*}{\partial \varphi}\right)_{Mer.} = -\frac{1}{r}\left(\frac{\partial w^*}{\partial \varphi}\right)^2_{Mer.} - \frac{1}{r}\frac{dr}{dx}\left(\frac{\partial w^*}{\partial \varphi}\right)_{Mer.} - \frac{1}{r\gamma M_e^2}\left(\frac{1}{p_e}\frac{\partial^2 p_e}{\partial \varphi^2}\right)_{Mer.} \qquad \text{(II-4)}$$

For bodies with conical symmetry where $\frac{\partial}{\partial x} = 0$, eq. II-3 becomes

$$\frac{1}{r}\left(\frac{\partial w}{\partial \varphi}\right)^2 + \frac{1}{r}\frac{dr}{dx}u\frac{\partial w}{\partial \varphi} + \frac{1}{\rho r}\frac{\partial^2 p}{\partial \varphi^2} = 0 \qquad \text{(II-5)}$$

Written in non-dimensional form, eq. II-5 becomes

$$\left(\frac{\partial w^*}{\partial \varphi}\right)^2_{Mer.} + \sin\eta_c\left(\frac{\partial w^*}{\partial \varphi}\right)_{Mer.} + \frac{1}{\gamma M_e^2}\left(\frac{1}{p_e}\frac{\partial^2 p_e}{\partial \varphi^2}\right)_{Mer.} = 0 \qquad \text{(II-6)}$$

Eq. II-6 is quadratic and is readily solved

$$\left(\frac{\partial w^*}{\partial \varphi}\right)_{Mer.} = -\frac{\sin\eta_c}{2} + \sqrt{\frac{\sin^2\eta_c}{4} - \frac{1}{\gamma M_e^2}\left(\frac{1}{p_e}\frac{\partial^2 p_e}{\partial \varphi^2}\right)_{Mer.}} \qquad \text{(II-7)}$$

valid for $\frac{\sin^2\eta_c}{4} - \frac{1}{\gamma M_e^2}\left(\frac{1}{p_e}\frac{\partial^2 p_e}{\partial \varphi^2}\right)_{Mer.} \geq 0$

For bodies with cylindrical symmetry, eq. II-6 becomes

$$\left(\frac{\partial w^*}{\partial \varphi}\right)^2_{Mer.} + \frac{1}{\gamma M_e^2}\left(\frac{1}{p_e}\frac{\partial^2 p_e}{\partial \varphi^2}\right)_{Mer.} = 0 \qquad \text{(II-8)}$$

the solution of which is

$$\left(\frac{\partial w^*}{\partial \varphi}\right)_{Mer.} = \left[-\frac{1}{\gamma M_e^2}\left(\frac{1}{p_e}\frac{\partial^2 p_e}{\partial \varphi^2}\right)_{Mer.}\right]^{1/2} \qquad \text{(II-9)}$$

provided that the term in the radical sign is $\geq 0$.

It is possible now to write the momentum and energy integral equations valid for different configurations.

For a curved flare:

$$\frac{d\theta}{dx} = -\left[ \left( \bar{H} + 2 \right) \frac{1}{u_e} \frac{du_e}{dx} + \frac{1}{\rho_e} \frac{d\rho_e}{dx} + \frac{1}{r} \frac{dr}{dx} \right] \theta -$$

$$- \frac{1}{r} \left( \frac{\partial w^*}{\partial \varphi} \right)_{Mer.} \int_o^\delta \frac{\rho}{\rho_e} \left( 1 - \frac{u}{u_e} \right) dy + {}^{C_f}/_2 \text{ - (Momentum Equation)} \qquad \text{(II-10)}$$

$$\frac{d\Phi}{dx} = -\left[ \frac{1}{u_e} \frac{du_e}{dx} + \frac{1}{\rho_e} \frac{d\rho_e}{dx} + \frac{1}{r} \frac{dr}{dx} \right] \Phi - \frac{1}{r} \left( \frac{\partial w^*}{\partial \varphi} \right)_{Mer.} \int_o^\delta \frac{\rho}{\rho_e} \left( 1 - \frac{H^*}{H_e^*} \right) dy -$$

$$- \frac{q_w}{\rho_e u_e H_e^*} \text{ - (Energy equation)} \qquad \text{(II-11)}$$

For a cone:

$$\frac{d\theta}{dx} = -\frac{\theta}{x} - \frac{1}{x \sin \eta_c} \left( \frac{\partial w^*}{\partial \varphi} \right)_{Mer.} \int_o^\delta \frac{\rho}{\rho_e} \left( 1 - \frac{u}{u_e} \right) dy + {}^{C_f}/_2 \text{ (Momentum Eq.)} \qquad \text{(II-12)}$$

$$\frac{d\Phi}{dx} = -\frac{\Phi}{x} - \frac{1}{x \sin \eta_c} \left( \frac{\partial w^*}{\partial \varphi} \right)_{Mer.} \int_o^\delta \frac{\rho}{\rho_e} \left( 1 - \frac{H^*}{H_e^*} \right) dy - \frac{q_w}{\rho_e u_e H_e^*} \text{ (Energy Eq.)} \qquad \text{(II-13)}$$

For a cylinder:

$$\frac{d\theta}{dx} = -\frac{1}{r_{cyl.}} \left( \frac{\partial w^*}{\partial \varphi} \right)_{Mer.} \int_o^\delta \frac{\rho}{\rho_e} \left( 1 - \frac{u}{u_e} \right) dy + {}^{C_f}/_2 \text{ (Momentum Eq.)} \qquad \text{(II-14)}$$

$$\frac{d\Phi}{dx} = - \frac{1}{r_{cyl.}} \left( \frac{\partial w^*}{\partial \varphi} \right)_{Mer.} \int_o^{\delta} \frac{\rho}{\rho_e} \left( 1 - \frac{H^*}{H_e^*} \right) dy - \frac{q_w}{\rho_e u_e H_e^*} \qquad \text{(II-15)}$$

In eq. II-4, the term $\left( \frac{\partial^2 p_e}{\partial \varphi^2} \right)_{Mer.}$ can be evaluated.

The pressure distribution on a body of revolution can be represented to second-order approximation by the following equation:

$$p_e = p_z + A\ \alpha \cos \varphi + D\ \alpha^2 + B\ \alpha^2 \cos 2\varphi \qquad \text{(II-16)}$$

where $\varphi = 0°$ represents the leeward side, $p_z$ is the static pressure at zero angle of attach. A, D, and B are constants which depend on the free stream Mach number and the body semivertex angle, and $\alpha$ is the angle of attack. If the peripheral pressure distribution is known experimentally, then it is possible to obtain the values of the constants from the approximate values of the pressure at different peripheral angles, for instance $\varphi = 0°$, $\varphi = 90°$, and $\varphi = 180°$.

Differentiating eq. II-16 twice with respect to $\varphi$, we get

$$\frac{\partial^2 p_e}{\partial \varphi^2} = - A\ \alpha \cos \varphi - 4\ B\ \alpha^2 \cos 2\varphi \qquad \text{(II-17)}$$

On the windward side of the meridian plane ($\varphi = 180°$), equation II-17 becomes

$$\left( \frac{\partial^2 p_e}{\partial \varphi^2} \right)_{Mer.} = A\ \alpha - 4\ B\ \alpha^2 \qquad \text{(II-18)}$$

Alternatively, the term $\left( \frac{\partial^2 p_e}{\partial \varphi^2} \right)_{Mer.}$ could be obtained assuming a Newtonian approximation for the pressure distribution

$$\frac{p_e}{(p_e)_{Mer.}} = \bar{p}_e = \frac{(\sin \eta_c \cos \alpha + \sin \alpha \cos \eta_c \cos \varphi)^2}{(\sin \eta_c \cos \alpha + \sin \alpha \cos \eta_c)^2} \qquad \text{(II-19)}$$

where $\varphi = 0^{o}$ represents the windward side.

Differentiating twice with respect to $\varphi$

$$\frac{\partial^2 \bar{p}_e}{\partial \varphi^2} = -2 \frac{\left[\sin \eta_c \cos \eta_c \sin \alpha \cos \alpha \cos \varphi - \cos^2 \eta_c \sin^2 \alpha \left(\sin^2 \varphi - \cos^2 \varphi\right)\right]}{\sin^2 (\alpha + \eta_c)} \qquad \text{(II-20)}$$

At the meridian plane

$$\left( \frac{\partial^2 \bar{p}_e}{\partial \varphi^2} \right)_{Mer.} = \left( \frac{1}{p_e} \frac{\partial^2 p_e}{\partial \varphi^2} \right)_{Mer.} = -2 \frac{(\sin \eta_c \cos \eta_c \sin \alpha \cos \alpha + \cos^2 \eta_c \sin^2 \alpha)}{\sin^2 (\alpha + \eta_c)} \qquad \text{(II-21)}$$

III. Application of power law velocity profile and Crocco-relation

In order to solve the boundary layer equations, some assumptions must be formulated with regard to the velocity, density and enthalpy profiles.

A power law velocity profile is assumed to be valid, i.e.

$$\frac{u}{u_e} = \left( y/\delta \right)^{1/N} \qquad \text{(III-1)}$$

On cones and cylinders, N can be set equal to a constant as it has been done in several analyses in axisymmetric or two dimensional flows, and it is considered a fairly good approximation of the actual profile. The assumption of the power profile validity in the laminar sublayer near the wall, instead of a linear profile, is perfectly acceptable due to the small contribution of this portion of the boundary layer to the integrals for $\theta$ and $\delta^*$ (Ref. 5).

On compression flares, N is taken as a variable. Persh, in Ref. 5, shows that the value of N is directly related to the variation of $R_{e_\theta}$. A plot of N versus $R_{e_\theta}$ shows good agreement with experimental results. The resulting

curve (Fig. 3 of Ref. 5) can be approximated as follows without introducing appreciable errors

$$R_{e_\theta} = 12\, e^N \qquad \text{(III-2)}$$

as it can be seen in Fig. 3. (Fig. 3)

It is possible then to set up a power correlation

$$R'_{e_\theta} = K\, e^N \qquad \text{(III-2A)}$$

where K is a constant depending on the value of $R'_{e_\theta}$ and on the power law assumption at the beginning of the flare, and the reference quantities are used to account for compressibility and heat transfer (Fig. 4). The Crocco (Fig. 4) Relation, modified as in Ref. 14, is used for the enthalpy profile and it is written as in Ref. 2, i.e. in terms of stagnation enthalpy to account for real gas effects.

$$\frac{H^*}{H^*_e} = (1-C)\,\frac{u}{u_e} + C\left(\frac{u}{u_e}\right)^2 \qquad \text{(III-3)}$$

where C is a constant that can be obtained by satisfying the initial values of the momentum and energy thickness integral parameters.

The static enthalpy profile can then be obtained

$$H = H_w + (H_e - H_w)\,\frac{u}{u_e} \qquad \text{(III-4)}$$

$$h + \tfrac{1}{2}u^2 = H_w + H^*_e\,\frac{u}{u_e} \qquad \text{(III-5)}$$

$$h = H_w + H^*_e\,\frac{u}{u_e} - \tfrac{1}{2}u^2 \qquad \text{(III-6)}$$

$$\frac{h}{h_e} = \frac{H_w}{h_e} + \frac{H^*_e}{h_e}\,\frac{u}{u_e} - \frac{u_e^2}{2h_e}\left(\frac{u}{u_e}\right)^2 \qquad \text{(III-7)}$$

The modified profile is then

$$\frac{h}{h_e} = \frac{H_w}{h_e} + (1-C)\,\frac{H^*_e}{h_e}\,\frac{u}{u_e} + \left(C - \frac{u_e^2}{H^*_e}\right)\frac{H^*_e}{2h_e}\left(\frac{u}{u_e}\right)^2 \qquad \text{(III-8)}$$

The density profile based on the assumption of zero normal pressure gradient is

$$\frac{\rho}{\rho_e} = \frac{h_e}{h} \tag{III-9}$$

## IV. Skin Friction and Heat Transfer

The skin friction method of Reference 5 is used with the modification that T', the reference temperature, is used for the Reynolds number based on the length and on the boundary layer thickness.

$$C_f/2 = \left(\frac{1}{20N}\right)^{\frac{N-1}{N+1}} \left(\frac{1}{Re'_\delta}\right)^{\frac{2}{N+1}} \left(\frac{T_\infty}{T_L}\right)^{\frac{N-2.52}{N+1}} \tag{IV-1}$$

where

$$Re'_\delta = \frac{\rho' u_e \delta}{\mu'} \tag{IV-2}$$

$$\frac{T_\infty}{T_L} = \left[ \frac{Re'_\delta}{\left(\frac{Re'}{2}\right)^{\frac{N+1}{N+3}} \left(\frac{\delta}{\theta}\right)^{\frac{N+1}{N+3}} \left(\frac{N+3}{N+1}\right)^{\frac{N+1}{N+3}} \left(\frac{1}{20N}\right)^{\frac{N-1}{N+3}}} \right]^{\frac{N+3}{N-2.52}} \tag{IV-3}$$

and

$$Re' = \frac{\rho' u_e s_1}{\mu'} \tag{IV-4}$$

The value obtained from Eq. IV-1 is compared with values obtained in Refs. 3 and 16 for a cold wall in hypersonic stream and it is in good agreement (Fig. 5). (Fig. 5)

$T'$ is obtained from the reference enthalpy definition (Ref. 15)

$$\frac{h'}{h_e} = 1 + 0.035\, M_e^2 + 0.45 \left( \frac{H_w}{h_e} - 1 \right) \qquad \text{(IV-5)}$$

A modified Reynolds analogy is used to obtained the value of the heat transfer (Ref. 2)

$$\frac{q_w}{\rho_e u_e H_e^*} = \frac{C-1}{2} \quad C_f \quad Pr^{-2/3} \qquad \text{(IV-6)}$$

The initial value of the momentum thickness $\theta$ is obtained from Reshotko and Tucker flat plate formula evaluated at the beginning of the body or compression surface (Ref. 11)

$$\theta_i = \frac{0.0259 \left( \frac{T_{o_e}}{T_e} \right)^{0.311} x^{0.823}}{\left( \frac{T}{T_e} \right)^{0.602} \left( \frac{M_{e_o} a_o}{\nu_o} \right)^{0.177}} \qquad \text{(IV-7)}$$

On a conical or cylindrical surface the ratios $\frac{\theta}{\delta}$, and $\frac{\delta^*}{\delta}$ are constant, and for a given power law exponent $N_i$, wall temperature and Mach number, using Persh & Lee tables (Ref. 18) for compressible turbulent flow, $\delta_i$ and $\delta_i^*$ can be obtained once the initial value of the momentum thickness is known. Alternatively, using the values of $\theta_i$ and $N_i$, $\delta_i$ and $\delta_i^*$ can be obtained from the integral parameters equations [Eqs. I-10 and I-11].

V. Method of Solutions:

The equations obtained in the past sections constitute a full set necessary to obtain a solution. The momentum and energy integral equations are solved numerically by a finite-difference method as indicated below.

1. The following conditions are given:
   Local stagnation pressure and temperature, boundary conditions for p(x) and $\left(\frac{T_w}{T_{o_\infty}}\right)$, initial conditions $N_i$ and $\theta_i$, body geometry.
2. Compute $\delta_i$ and $\delta_i^*$ (from Eqs. I-10, I-11)
3. Compute $(C_f/2)_i$ (Eq. IV-1).
4. Increment body length $x_{i+1} = x_i + \Delta x$.
5. Solve momentum integral equations in the streamwise and peripheral directions and energy integral equation.
6. Obtain new $\theta$ and $\Phi$.
7. Obtain new N.
8. Choose $\delta$ and solve integral parameters for $\theta$ and $\Phi$.
9. Compare $\theta$ and $\Phi$ from integral equations and integral parameters.
10. If no agreement obtained, perturb $\delta$ through iterations until agreement is reached.
11. Repeat at next station up to the end of the body.

The solutions obtained are compared with the experiment of Ref. 6 performed on a yawed cone and the experiment of Ref. 7 on a curved flare at zero angle of attack (neglecting the inviscid contribution for the latter), and the agreement is good.

VI. Comparison with experimental results (cone):

A comparison is made between the theory developed and the experiment in Ref. 6 on the windward side of the meridian plane. Ref. 6 tabulates the experimental results obtained for the boundary layer parameters on a yawed cone placed in a turbulent compressible flow. The same initial conditions, i.e. Mach number, stagnation temperature and pressure, and the same ratio of angle of attach to semivertex cone angle, are used.

The pressure distribution in the peripheral direction reported in Ref. 6 is used to set up a system of three linear algebraic equations to determine the constants A, D and B in Eq. II-16 needed to find the value of $\left(\partial^2 p_e/\partial\varphi^2\right)_{Mer.}$, while the Mach number distribution in the boundary layer is used to obtain, by means of the Crocco relation, the power law exponent 1/N. The Newtonian approximation for the pressure distribution (Eq. II-21) is also used alternatively, obtaining no appreciable difference.

The boundary layer parameters $\delta, \delta^*$ and $\theta$ are therefore calculated. The calculations are performed with and without the cross flow term in order to study its direct effect on these parameters. The constant C of the modified Crocco relation is evaluated, but in a set of calculations, it is set equal to zero in order to compare the two results. As it can be seen from Figs. 6-9, the results for C = 0 and C = constant are exactly the same, as it is expected

(Figs.6-9)

since the standard Crocco relation applies well on a cone. (Note that setting C=0 the parameters $\theta$ and $\Phi$ become identically equal).

The experimental values of Ref. 6 for $\delta$, $\delta^*$ and $\theta$ are

$$\delta = 0.155"$$
$$\delta^* = 0.04"$$
$$\theta = 0.0095"$$

The present results are

$$\delta = 0.1581"$$
$$\delta^* = 0.0394" \qquad \text{for } \left(\frac{\partial w^*}{\partial \varphi}\right)_{\text{Mer.}} = \text{const.}$$
$$\theta = 0.0088"$$

and

$$\delta = 0.1975"$$
$$\delta^* = 0.0451" \qquad \text{for } \left(\frac{\partial w^*}{\partial \varphi}\right)_{\text{Mer.}} = 0$$
$$\theta = 0.01098$$

The cross flow adjustment, where the quantity $\left(\frac{\partial w^*}{\partial \varphi}\right)_{\text{Mer.}}$ is constant in the streamwise direction on a cone, gives a value for $\delta$ within 2% of the experimental value, a value for $\delta^*$ within 1.5% and a value for $\theta$ within 7%, while, ignoring the cross flow, the values for $\delta$, $\delta^*$ and $\theta$ are off by 27.4%, 12.7%, and by 15.5% respectively.

The results with and without crossflow differ by about 20%.

## VII. Comparison with experimental results (compression flare):

In Ref. 7, an experimental investigation of hypersonic turbulent boundary layer in large adverse pressure gradient on an axisymmetric flare at zero angle of attack is treated. The experiments are performed at a free stream Mach

Number of 5.75. On the flare, due to the high pressure rise, adverse pressure gradients have a large normal variation across the boundary layer, which is not accounted for by boundary layer theory that sets the normal pressure gradient equal to zero. Therefore Hoydysh and Zakkay, as well as others (see Refs. 2, 10 and 17), take into account the inviscid component of the boundary layer parameters, and present measured data and viscous data. The measured data are to be understood as the superposition of the inviscid and viscous components. Since in the present analysis the static pressure in the normal direction is assumed constant throughout the boundary layer, the comparison is made with the viscous data of Ref. 7. The term due to the cross flow is set equal to zero (no cross flow present on the flares at $\alpha=0$). In this case the momentum and energy equations reduce to the equations of Ref. 2. The results obtained (Figs.10-15) are in satisfactory agreement with the experimental data as well as with previous theoretical investigations by Sasman & Cresci (Ref. 12) and Reshotko & Tucker (Ref. 11). (Figs.10-15)

The calculations of the boundary layer parameters are repeated for $\alpha=10^{o}$ on the windward side of the model. In this case the term due to the crossflow $\left(\frac{\partial w^{*}}{\partial \varphi}\right)_{Mer.}$ is a function of the streamwise distance s', measured from the beginning of the flare. The results are plotted in Figs. 16-20 and compared to the ones obtained by setting $\left(\frac{\partial w^{*}}{\partial \varphi}\right)_{Mer.} = 0$ for the same inviscid distribution to determine again the effect of the cross flow. (Figs.16-20)

The values of $\delta$, $\delta^{*}$, and $\theta$, taking into consideration the crossflow, are 20-25% lower than those without crossflow, while the form factor H, except for a slight variation at the beginning of the flare, is identical in both cases. In Fig. 21, the mass flux defect due to the crossflow is shown. (Fig. 21)

VIII. Cylinder investigation.

The boundary layer parameters are calculated for a hollow cylinder at an angle of attack and the results plotted in Figs. 22-25 and compared with values obtained setting $\left(\frac{\partial w^*}{\partial \varphi}\right)_{Mer.} = 0$. It is found that the crossflow has a damping effect on the growth of the parameters along the surface, and, beginning at x = 17", they approach a constant value up to the end of the cylindrical surface (x=35"). (Figs. 22-25)

Conclusion

A method for calculating the compressible turbulent boundary layer undergoing both adverse pressure gradient and crossflow along a plane of symmetry has been presented.

While the method allows one to obtain the boundary layer parameters such as $\delta, \delta^*$ and $\theta$, it cannot predict separation. The method in addition assumes zero normal pressure gradient, however, the contribution due to $\partial p/\partial y$ could be added as has been demonstrated in Ref. 9.

The method of solution is simple and the numerical calculations do not require a long computer time. The program can be used for any body shape and any set of initial and boundary conditions. Comparison with experiments and previous theories are made in absence of crossflow to show the validity of the present method. Due to the paucity of experiments on the subject, only the experiment of Ref. 6 that involves crossflow is compared to the

present theory.

The present authors will present in part two a detailed experimental study in order to verify the present analysis.

## REFERENCES


1. Cooke, J.C., and Hall, M.G., "Boundary Layers in Three Dimensions," Progress in Aeronautical Sciences, Vol. 2, "Boundary Layer Problems," Edited by Antonio Ferri, D. Küchemann, L.H.G. Sterne, Pergamon Press 1962.

2. Miller, Leonard D., "Predicting Turbulent Compressible Boundary Layers in Strong Adverse Pressure Gradient", AIAA Paper No. 67-196, Jan. 1967.

3. Cresci, R.J., Economos, C., and Libby, P.A., "Theoretical Analyses of Some Three-Dimensional Boundary Layers with particular Applicability to Hypersonic Inlets," Part III Technical Report No. 304, General Applied Science Laboratories, Inc., Dec. 1962.

4. Braun, Willis H., "Turbulent Boundary Layer on a Yawed Cone in a Supersonic Stream," Technical Report R-7, NASA, 1959.

5. Persh, Jerome, "A Theoretical Investigation of Turbulent Boundary Layer Flow with Heat Transfer at Supersonic and Hypersonic Speeds," NAVORD Report 3854, Aeroballistic Research Report 258, U.S. Naval Ordinance Laboratory, White Oak, Maryland, May, 1955.

6. Rainbird, W.J., "Turbulent Boundary Layer Growth and Separation on a Yawed Cone," AIAA Journal, p. 2410, Dec. 1968.

7. Hoydysh, W.G., and Zakkay, V., "An Experimental Investigation of Hypersonic Turbulent Boundary Layers in Adverse Pressure Gradient," AIAA Journal, p. 105, Jan. 1969.

8. Bradley, R.G., "Approximate Solutions for Compressible Turbulent Boundary Layers in Three-Dimensional Flow," AIAA Journal, p. 859, May 1968.

9. Zakkay, V., "Pressure and Laminar Heat Transfer Results in Three-Dimensional Hypersonic Flow," WADC Technical note 58-152, ASTIA Document No. 155-679, Polytechnic Institute of Brooklyn, Department of Aeronautical Engineering and Applied Mechanics, Sept. 1958.

10. Stroud, J.F., and Miller, L.D., "An Experimental and Analytical Investigation of Hypersonic Inlet Boundary Layers," Technical Report, AFFDL TR-65-123, August 1965.

11. Reshotko, E. and Tucker, M., "Approximate Calculation of the Compressible Turbulent Boundary Layer with Heat Transfer and Arbitrary Pressure Gradient,: NACA TN 4154, December 1957.

12. Sasman, P.K., and Cresci, R.J., "Compressible Turbulent Boundary Layer with Pressure Gradient and Heat Transfer," AIAA J. 1, 19-25 (1966).

13. Sommer, S.C. and Short, B.J., "Free-Flight Measurements of Turbulent Boundary-Layers Skin Friction in the Presence of Severe Aerodynamic Heating at Mach Numbers from 2.8 to 7.0, NACA TN 3391, 1955.

14. Cohen, N.B., "A Method for Computing Turbulent Heat Transfer in the Presence of a Streamwise Pressure Gradient for Bodies in High-Speed Flow," NASA Memo 1-2-5-L, 1959.

15. Eckert, E.R.G., "Survey on Heat Transfer at High Speeds," WADC, TR 54-70, 1954.

16. Braun, W.H., "Turbulent Boundary Layer on a Yawed Cone in a Supersonic Stream," NACA TN 4208, Jan. 1958.

17. McLafferty, G.H., and Barber, R.E., "The Effect of Adverse Pressure Gradients on the Characteristics of Turbulent Boundary Layers in Supersonic Streams". J. Aerospace Sci., 29, 1-11, 1962.

18. Persh, Jerome and Roland, Lee,"Tabulation of Compressible Turbulent Boundary Layer Parameters," NAVORD Report 4282, Aeroballistic Research Report 337, May 1, 1956, U.S. Naval Ordnance Lab., White Oak, Maryland.

## APPENDIX I

### Derivation of Momentum Integral equation in the Streamwise Direction.

The steady boundary layer momentum equation in the streamwise direction is:

$$\rho\left(u\frac{\partial u}{\partial x}+v\frac{\partial u}{\partial y}+\frac{w}{r}\frac{\partial u}{\partial \varphi}-\frac{1}{r}\frac{dr}{dx}w^2\right)=-\frac{\partial p}{\partial x}+\frac{\partial}{\partial y}\left(\mu\frac{\partial u}{\partial y}\right) \tag{1-1}$$

and the continuity equation is:

$$\frac{\partial}{\partial x}(\rho r u)+\frac{\partial}{\partial \varphi}(\rho w)+\frac{\partial}{\partial y}(\rho r v)=0 \tag{1-2}$$

At $y=0$, $u=v=w=0$ and at $y=\delta$, $u=u_e$ and $v_e=w_e=0$, therefore the boundary conditions for eq. 1-1 are:

$$\rho_e u_e\frac{du_e}{dx}=-\frac{\partial p}{\partial x} \tag{1-3}$$

$$\left[\frac{\partial}{\partial y}\left(\mu\frac{\partial u}{\partial y}\right)\right]_{y=0}=\frac{\partial p}{\partial x} \tag{1-4}$$

In order to derive the integral form of eq. 1-1 we make use of the continuity eq. 1-2, from which

$$v=-\frac{1}{\rho r}\int_o^y\left[\frac{\partial}{\partial x}(\rho r u)+\frac{\partial}{\partial \varphi}(\rho w)\right]dy \tag{1-5}$$

Substituting for v in eq. 1-1, integrating term by term from 0 to $\delta$, and using the boundary conditions

$$\int_o^\delta \rho u\frac{\partial u}{\partial x}dy-\int_o^\delta\left\{\frac{1}{r}\int_o^y\left[\frac{\partial}{\partial x}(\rho r u)+\frac{\partial}{\partial \varphi}(\rho w)\right]dy\right\}\frac{\partial u}{\partial y}dy+\int_o^\delta\frac{\rho w}{r}\left(\frac{\partial u}{\partial y}\right)dy$$

$$-\int_o^\delta\frac{\rho w^2}{r}\frac{dr}{dx}dy=\int_o^\delta\rho_e u_e\frac{du_e}{dx}dy+\int_o^\delta\frac{\partial}{\partial y}\left(\mu\frac{\partial u}{\partial y}\right)dy \tag{1-6}$$

The term $\int_o^\delta \frac{\partial u}{\partial y} \left\{ \int_o^y \left[ \frac{\partial}{\partial x}(\rho r u) + \frac{\partial}{\partial \varphi}(\rho w) \right] dy \right\} dy$ in eq. 1-6 can be integrated by parts

$$\int_o^\delta \left[ \frac{\partial u}{\partial y} \int_o^y \frac{\partial}{\partial x}(\rho r u)\, dy \right] dy = u_e \int_o^\delta \frac{\partial}{\partial x}(\rho r u) dy - \int_o^\delta u \frac{\partial}{\partial x}(\rho r u)\, dy \quad (1\text{-}7)$$

$$\int_o^\delta \left[ \frac{\partial u}{\partial y} \int_o^y \frac{\partial}{\partial \varphi}(\rho w) dy \right] dy = u_e \int_o^\delta \frac{\partial}{\partial \varphi}(\rho w) dy - \int_o^\delta u \frac{\partial}{\partial \varphi}(\rho w) dy \quad (1\text{-}8)$$

Substituting in eq. 1-1

$$\int_o^\delta \rho u \frac{\partial u}{\partial x} dy - \frac{1}{r} \left\{ u_e \int_o^\delta \frac{\partial}{\partial x}(\rho r u)\, dy - \int_o^\delta u \frac{\partial}{\partial x}(\rho r u) dy + u_e \int_o^\delta \frac{\partial}{\partial \varphi}(\rho w)\, dy \right.$$
$$\left. - \int_o^\delta u \frac{\partial}{\partial \varphi}(\rho w)\, dy \right\} + \int_o^\delta \frac{\rho w}{r} \left( \frac{\partial u}{\partial y} \right) dy - \int_o^\delta \frac{\rho w^2}{r} \frac{dr}{dx} dy =$$
$$= \int_o^\delta \rho_e u_e \frac{du_e}{dx} dy + \int_o^\delta \frac{\partial}{\partial y} \left( \mu \frac{\partial u}{\partial y} \right) dy \quad (1\text{-}9)$$

Noting that

$$\frac{1}{r} \int_o^\delta u \frac{\partial}{\partial x}(\rho r u)\, dy = \int_o^\delta u \frac{\partial}{\partial x}(\rho u)\, dy + \frac{1}{r} \int_o^\delta \rho u^2 \frac{dr}{dx} dy \quad (1\text{-}10)$$

$$\left[ \frac{\partial}{\partial x}(\rho r u) \right] u_e = \frac{\partial}{\partial x}(\rho r u u_e) - \rho r u \frac{du_e}{dx} \quad (1\text{-}11)$$

that the cross flow velocity w is equal to zero at the meridian plane, and rearranging terms, eq. (1-9) becomes

$$\int_o^\delta \frac{\partial}{\partial x}(\rho u^2)\, dy - \frac{1}{r} \int_o^\delta \frac{\partial}{\partial x}(\rho r u u_e) dy + \frac{1}{r} \int_o^\delta \rho r u \frac{du_e}{dx} dy +$$
$$+ \frac{1}{r} \int_o^\delta \rho u^2 \frac{dr}{dx} dy - \frac{1}{r} \int_o^\delta \rho \left( \frac{\partial w}{\partial \varphi} \right)_{Mer.} (u_e - u)\, dy - \int_o^\delta \rho_e u_e \frac{du_e}{dx} dy =$$
$$= - \mu \left( \frac{\partial u}{\partial y} \right)_{y=0} \quad (1\text{-}12)$$

But $\frac{\partial}{\partial x}\left(\rho r u u_e\right) = r\frac{\partial}{\partial x}(\rho u u_e) + \rho w u_e \frac{dr}{dx}$ (1-13)

Interchanging the order of integration and differentation, noting that $\left(\frac{\partial w}{\partial \varphi}\right)_{Mer.}$ depends on the inviscid pressure distribution and therefore is independent of y, multiplying and dividing the left hand side of eq. (1-12) by $\rho_e u_e^2$, and substituting eq. (1-13) into eq. (1-12) then

$$\frac{d}{dx}\rho_e u_e^2 \int_o^\delta \frac{\rho u}{\rho_e u_e}\left(\frac{u}{ue} - 1\right) dy + \rho_e u_e^2 \frac{1}{r}\frac{dr}{dx}\int_o^\delta \frac{\rho u}{\rho_e u_e}\left(\frac{u}{ue} - 1\right) dy$$

$$+ \rho_e u_e \frac{du_e}{dx}\int_o^\delta \left(\frac{\rho u}{\rho_e u_e} - 1\right) dy - \frac{\rho_e u_e}{r}\left(\frac{\partial w}{\partial \varphi}\right)_{Mer.}\int_o^\delta \frac{\rho}{\rho_e}\left(1 - \frac{u}{u_e}\right) dy =$$

$$= -\mu\left(\frac{\partial u}{\partial y}\right)_{y=0} \quad (1\text{-}14)$$

Defining $\theta = \int_o^\delta \frac{\rho u}{\rho_e u_e}\left(1 - \frac{u}{u_e}\right) dy$ (1-15)

$$\delta^* = \int_o^\delta \left(1 - \frac{\rho u}{\rho_e u_e}\right) dy \quad (1\text{-}16)$$

$$\tau_o = \mu\left(\frac{\partial u}{\partial y}\right)_{y=0} \quad (1\text{-}17)$$

$$\bar{H} = \frac{\delta^*}{\theta} \quad (1\text{-}18)$$

substituting into eq. (1-14) and dividing by $\rho_e u_e^2$, the final result is:

$$\frac{d\theta}{dx} = -\left[\left(\bar{H} + 2\right)\frac{1}{ue}\frac{du_e}{dx} + \frac{1}{\rho_e}\frac{d\rho_e}{dx} + \frac{1}{r}\frac{dr}{dx}\right]\theta$$

$$- \frac{1}{ru_e}\left(\frac{\partial w}{\partial \varphi}\right)_{Mer.}\int_o^\delta \frac{\rho}{\rho_e}\left(1 - \frac{u}{u_e}\right) dy + C_{f/2} \quad (1\text{-}19)$$

## APPENDIX 2

### Derivation of the Energy Integral equation

Energy equation

$$\rho \left( u \frac{\partial H}{\partial x} + \frac{w}{r} \frac{\partial H}{\partial \varphi} + v \frac{\partial H}{\partial y} \right) = \frac{\partial}{\partial y} \left\{ \mu \left( \frac{\partial H}{\partial y} + \frac{1-Pr}{Pr} \frac{\partial h}{\partial y} \right) \right\} \tag{2-1}$$

For unity Prandtl number Eq. (2-1) becomes

$$\rho \left( u \frac{\partial H}{\partial x} + \frac{w}{r} \frac{\partial H}{\partial \varphi} + v \frac{\partial H}{\partial y} \right) = \frac{\partial}{\partial y} \left( \mu \frac{\partial H}{\partial y} \right) \tag{2-2}$$

Using continuity (Appendix 1, Eq. 1-2)

$$\rho \left\{ u \frac{\partial H}{\partial x} + \frac{w}{r} \frac{\partial H}{\partial \varphi} - \left[ \frac{1}{\rho r} \int_o^y \left( \frac{\partial}{\partial x} (\rho r u) + \frac{\partial}{\partial \varphi} (\rho w) \right) dy \right] \frac{\partial H}{\partial y} \right\} = \frac{\partial}{\partial y} \left( \mu \frac{\partial H}{\partial y} \right) \tag{2-3}$$

Integrating term by term throughout the boundary layer:

$$\int_o^\delta \left( \rho u \frac{\partial H}{\partial x} \right) dy + \int_o^\delta \left( \frac{\rho w}{r} \frac{\partial H}{\partial \varphi} \right) dy - \int_o^\delta \left\{ \frac{1}{r} \int_o^y \left[ \frac{\partial}{\partial x} (\rho r u) + \frac{\partial}{\partial \varphi} (\rho w) \right] dy \right\} \frac{\partial H}{\partial y} dy =$$

$$= \int_o^\delta \frac{\partial}{\partial y} \left( \mu \frac{\partial H}{\partial y} \right) dy \tag{2-4}$$

Integrating by parts the last term of the left-hand side of eq. (2-4)

$$\int_o^\delta \left[ \int_o^y \frac{\partial}{\partial x} (\rho r u)\, dy \right] \frac{\partial H}{\partial y} dy = H_e \int_o^\delta \frac{\partial}{\partial x} (\rho r u)\, dy - \int_o^\delta H \frac{\partial}{\partial x} (\rho r u) dy \tag{2-5}$$

and

$$\int_o^\delta \left[ \int_o^y \frac{\partial}{\partial \varphi} (\rho w) dy \right] \frac{\partial H}{\partial y} dy = H_e \int_o^\delta \frac{\partial}{\partial \varphi} (\rho w) dy - \int_o^\delta H \frac{\partial}{\partial \varphi} (\rho w) dy \tag{2-6}$$

Substituting eq.'s (2-5) and (2-6) into eq. (2-4) and again noting that the cross flow velocity w is equal zero at the meridian plane, we obtain

$$\int_o^\delta \rho u \frac{\partial H}{\partial x}\, dy - \frac{1}{r}\left\{ \int_o^\delta \left[ H_e - H \right] \frac{\partial}{\partial x} (\rho r u)\, dy + \int_o^\delta \left[ H_e - H \right] \rho \left( \frac{\partial w}{\partial \varphi} \right)_{Mer.} dy \right\} = q_w \qquad (2\text{-}7)$$

or

$$\int_o^\delta \frac{\partial}{\partial x} (\rho u H)\, dy - \frac{H_e}{r} \int_o^\delta \frac{\partial}{\partial x} (\rho r u)\, dy + \frac{1}{r} \int_o^\delta \rho u H \frac{dr}{dx}\, dy -$$

$$- \frac{1}{r} \int_o^\delta \left[ H_e - H \right] \rho \left( \frac{\partial w}{\partial \varphi} \right)_{Mer.} dy = q_w \qquad (2\text{-}8)$$

But

$H_e \frac{\partial}{\partial x} (\rho r u) = \frac{\partial}{\partial x} (\rho r u H_e) = r \frac{\partial}{\partial x} (\rho u H_e) + \rho u H_e \frac{dr}{dx}$ since the stagnation enthalpy is constant at the edge of the boundary layer.

Therefore eq. (2-8) becomes

$$\int_o^\delta \left[ \frac{\partial}{\partial x} (\rho u H - \rho u H_e) \right] dy + \frac{1}{r} \frac{dr}{dx} \int_o^\delta \rho u (H - H_e)\, dy =$$

$$= \frac{1}{r} \int_o^\delta (H_e - H) \rho \left( \frac{\partial w}{\partial \varphi} \right)_{Mer.} dy + q_w \qquad (2\text{-}9)$$

Interchanging order of integration and differentation, considering $\left( \frac{\partial w}{\partial \varphi} \right)_{Mer.}$ independent of y and noting that $\int_o^\delta \rho u (H - H_e)\, dy$ is only function of x at the meridian plane, eq. (2-9) becomes

$$\frac{d}{dx} \int_o^\delta \rho u (H - H_e)\, dy + \frac{1}{r} \frac{dr}{dx} \int_o^\delta \rho u (H - H_e)\, dy =$$

$$= \frac{1}{r} \left( \frac{\partial w}{\partial \varphi} \right)_{Mer.} \int_o^\delta \rho (H_e - H)\, dy + q_w \qquad (2\text{-}10)$$

or

$$\frac{d}{dx}\int_o^\delta \rho u\ (H_e - H)\ dy + \frac{1}{r}\frac{dr}{dx}\int_o^\delta \rho u\ (H_e - H)\ dy =$$

$$= -\frac{1}{r}\left(\frac{\partial w}{\partial \varphi}\right)_{Mer.}\int_o^\delta \rho\ (H_e - H)\ dy - q_w \qquad (2\text{-}11)$$

or

$$\frac{d}{dx}\int_o^\delta \rho u\left[(H_e - H_w) - (H - H_w\right]\ dy + \frac{1}{r}\frac{dr}{dx}\int_o^\delta \rho u\left[(H_e - H_w) - (H - H_w)\right]\ dy =$$

$$= -\frac{1}{r}\left(\frac{\partial w}{\partial \varphi}\right)_{Mer.}\int_o^\delta \rho\left[(H_e - H_w) - (H - H_w)\right]\ dy - q_w \qquad (2\text{-}12)$$

We have defined

$$H_e - H_w = H_e^* \text{ and } H - H_w = H^*$$

multiplying and dividing by $\rho_e u_e H_e^*$, eq. (2-12) becomes

$$\frac{d}{dx}\rho_e u_e H_e^* \int_o^\delta \frac{\rho u}{\rho_e u_e}\left(1 - \frac{H^*}{H_e^*}\right) dy + \frac{1}{r}\frac{dr}{dx}\rho_e u_e H_e^* \int_o^\delta \frac{\rho u}{\rho_e u_e}\left(1 - \frac{H^*}{H_e^*}\right) dy =$$

$$= -\frac{1}{r}\left(\frac{\partial w}{\partial \varphi}\right)_{Mer.}\rho_e u_e H_e^* \int_o^\delta \frac{\rho}{\rho_e u_e}\left(1 - \frac{H^*}{H_e^*}\right) dy - q_w \qquad (2\text{-}13)$$

and since we have defined

$$\Phi = \int_o^\delta \frac{\rho u}{\rho_e u_e}\left(1 - \frac{H^*}{H_e^*}\right) dy \qquad (2\text{-}14)$$

eq. (2-13) becomes

$$\frac{d}{dx}\left[\rho_e u_e H_e^* \Phi\right] + \frac{1}{r}\frac{dr}{dx}\rho_e u_e H_e^* \Phi =$$

$$= -\frac{1}{r}\left(\frac{\partial w}{\partial \varphi}\right)_{Mer.}\rho_e u_e H_e^* \int_o^\delta \frac{\rho}{\rho_e u_e}\left(1 - \frac{H^*}{H_e^*}\right) dy = q_w \qquad (2\text{-}15)$$

But

$$\frac{d}{dx}\left[\rho_e u_e H_e^* \Phi\right] = \rho_e u_e H_e^* \frac{d\Phi}{dx} + \rho_e H_e^* \frac{du_e}{dx}\Phi + u_e H_e^* \frac{d\rho_e}{dx}\Phi \qquad (2\text{-}16)$$

Therefore, substituting eq. (2-16) into eq. (2-15) and dividing by $\rho_e u_e H_e^*$, the final form of the energy integral eq. is

$$\frac{d\Phi}{dx} = -\left[\frac{1}{u_e}\frac{du_e}{dx} + \frac{1}{\rho_e}\frac{d\rho_e}{dx} + \frac{1}{r}\frac{dr}{dx}\right]\Phi - \frac{1}{ru_e}\left(\frac{\partial w}{\partial \varphi}\right)_{Mer.}\int_0^\delta \frac{\rho}{\rho_e}\left(1 - \frac{H^*}{H_e^*}\right)dy - \frac{q_w}{\rho_e u_e H_e^*} \qquad (2\text{-}17)$$

## LIST OF FIGURES

LIST OF FIGURES (cont.)

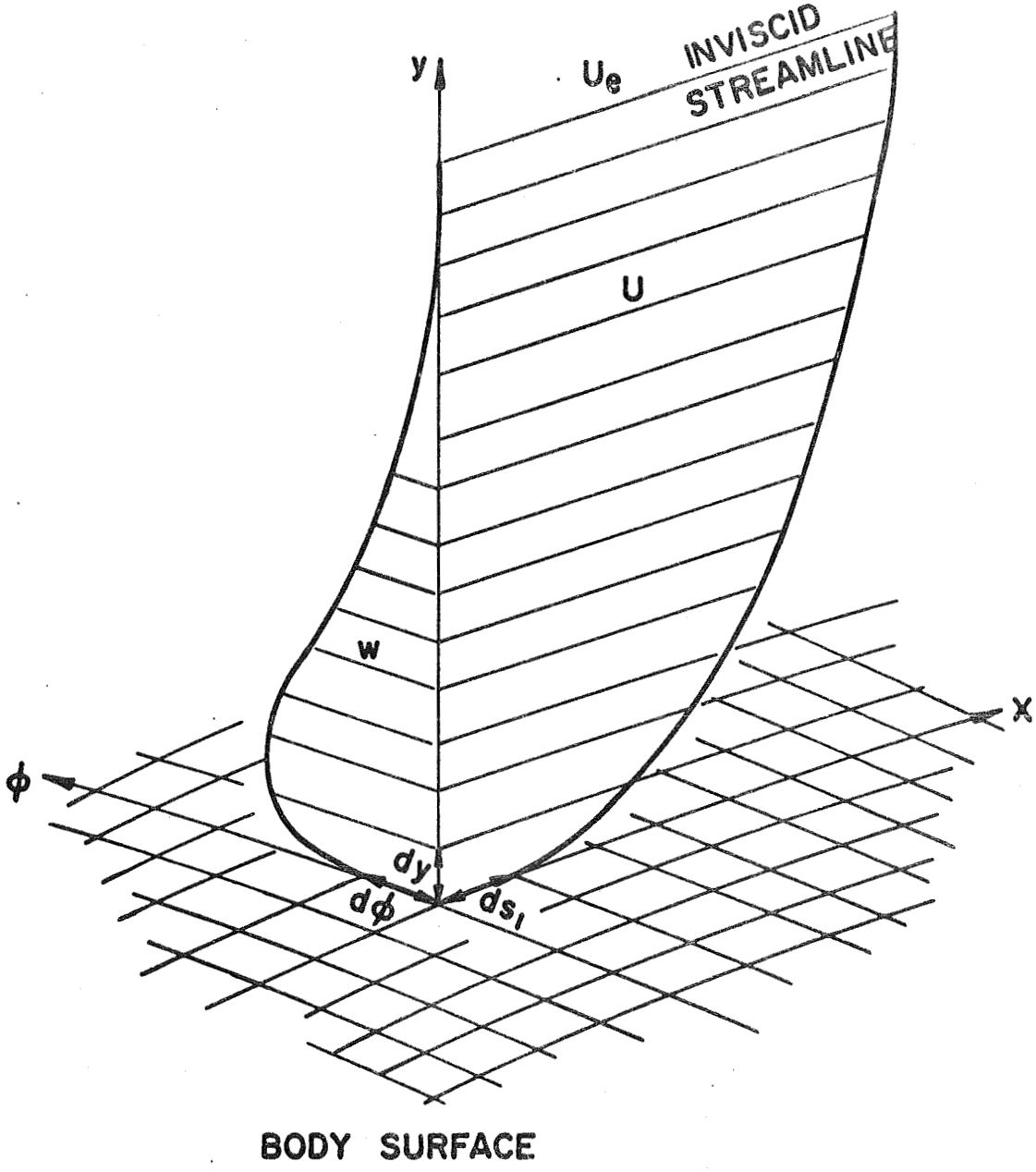


Fig. 1. Orthogonal System of Geodesic Coordinates

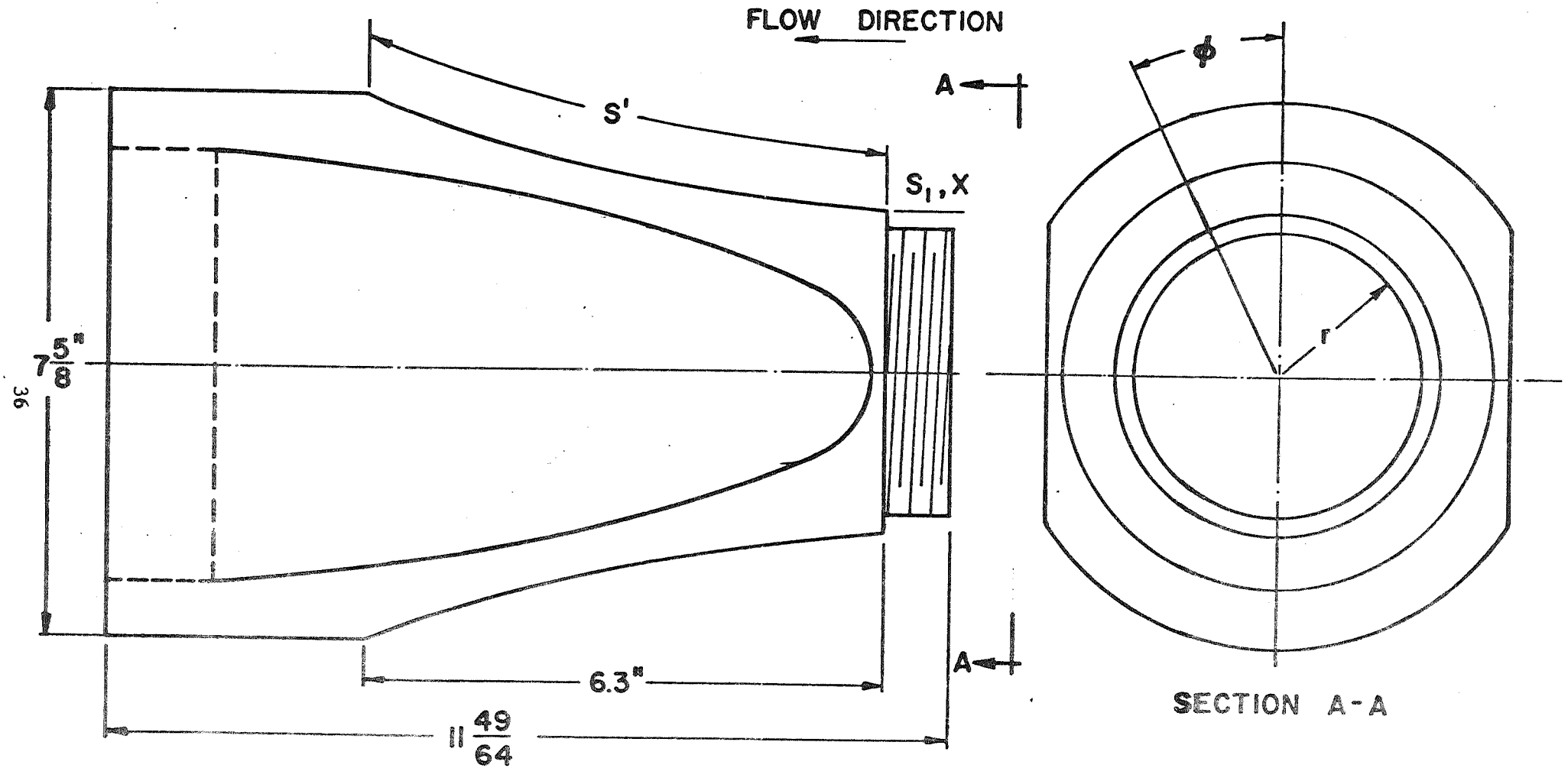


Fig. 2 Compression Flare Producing Crossflow

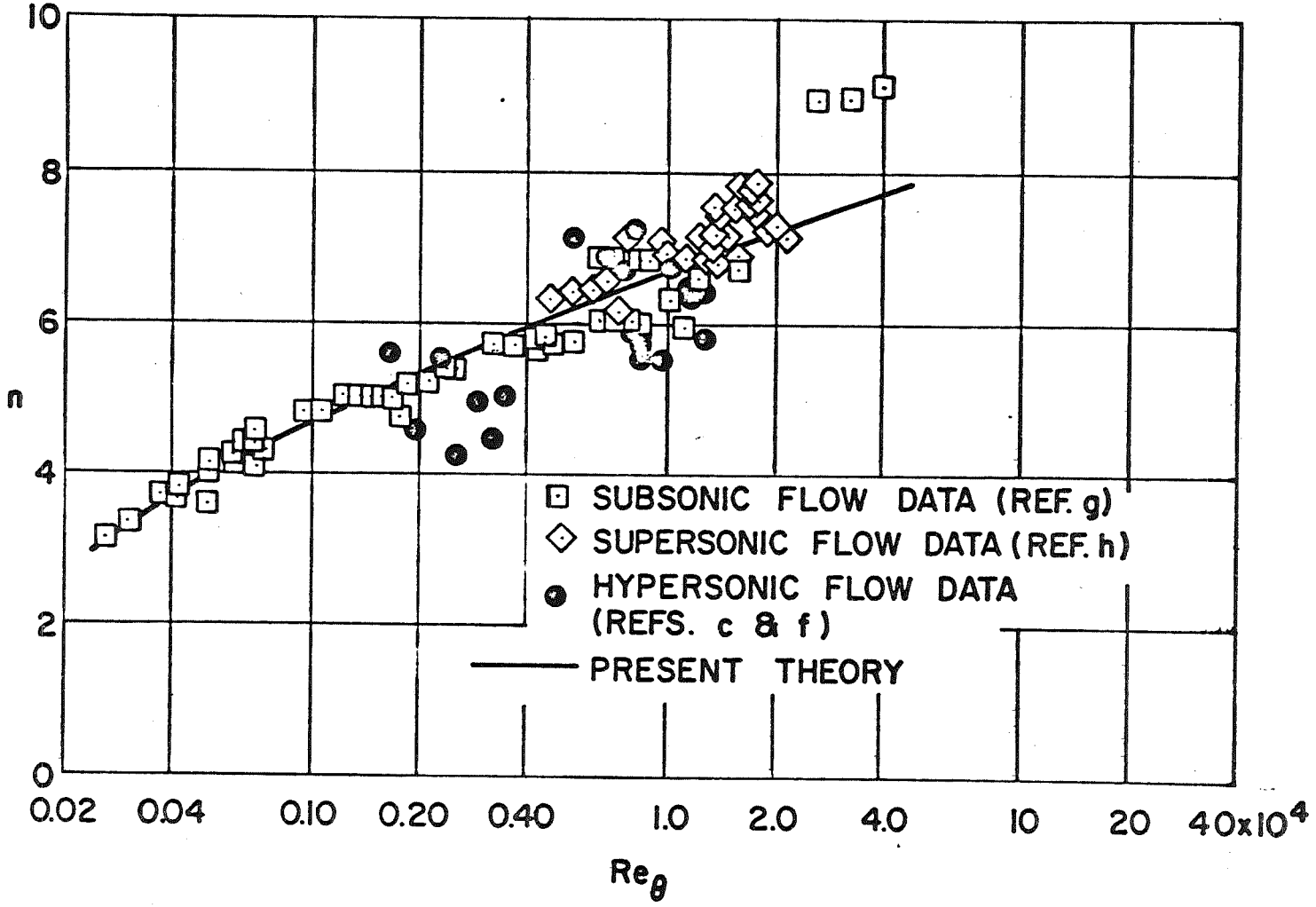


Fig. 3. Fig. 3 of Ref. 5- Variation of Turbulent Boundary Layer Velocity Profile Exponent (n) with Reynolds Number ($Re_\theta$).

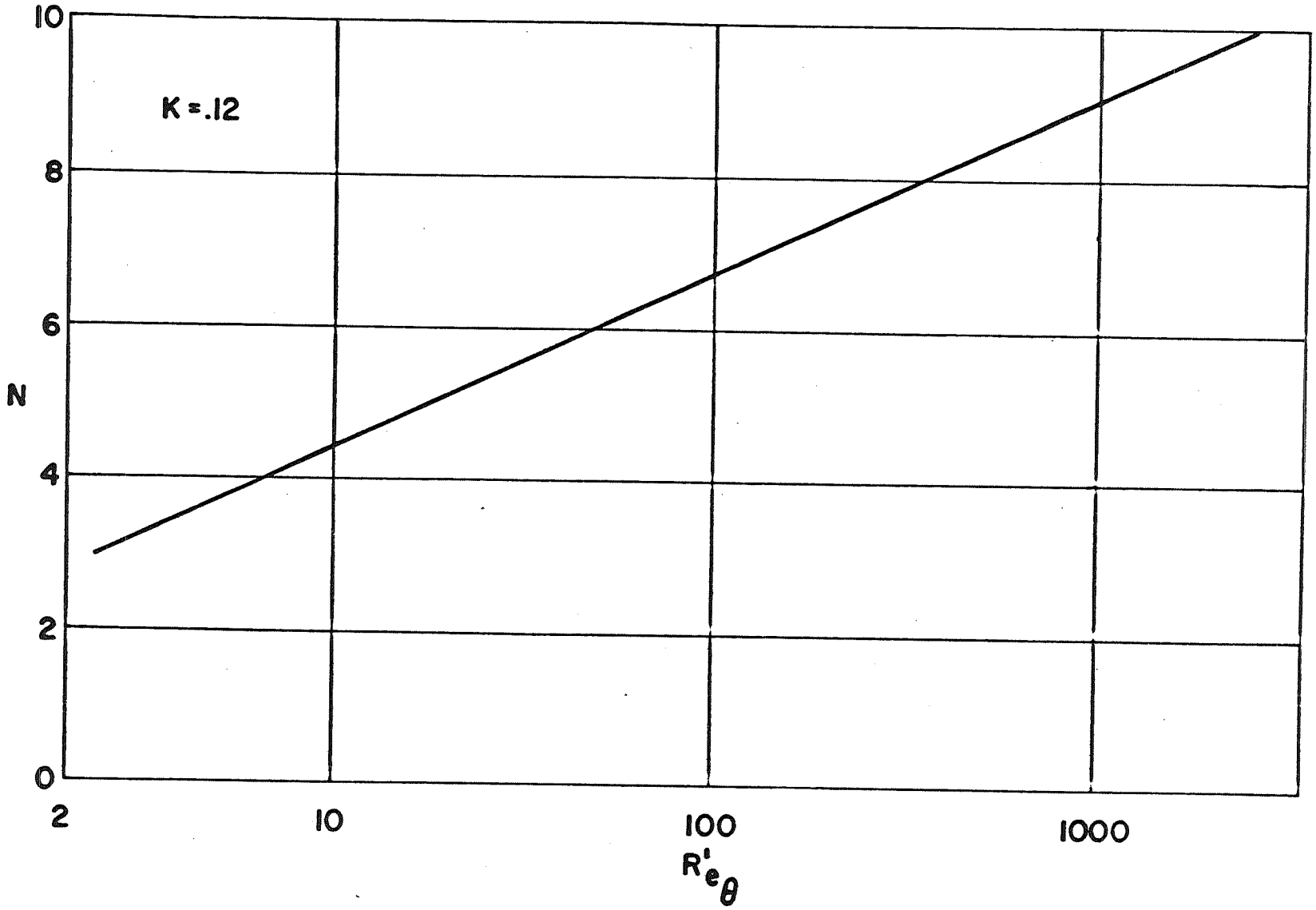


Fig. 4. Variation of Power Law Velocity Exponent (N) with Reference Reynolds Number ($Re_\theta$) for Curved Flare of Ref. 7

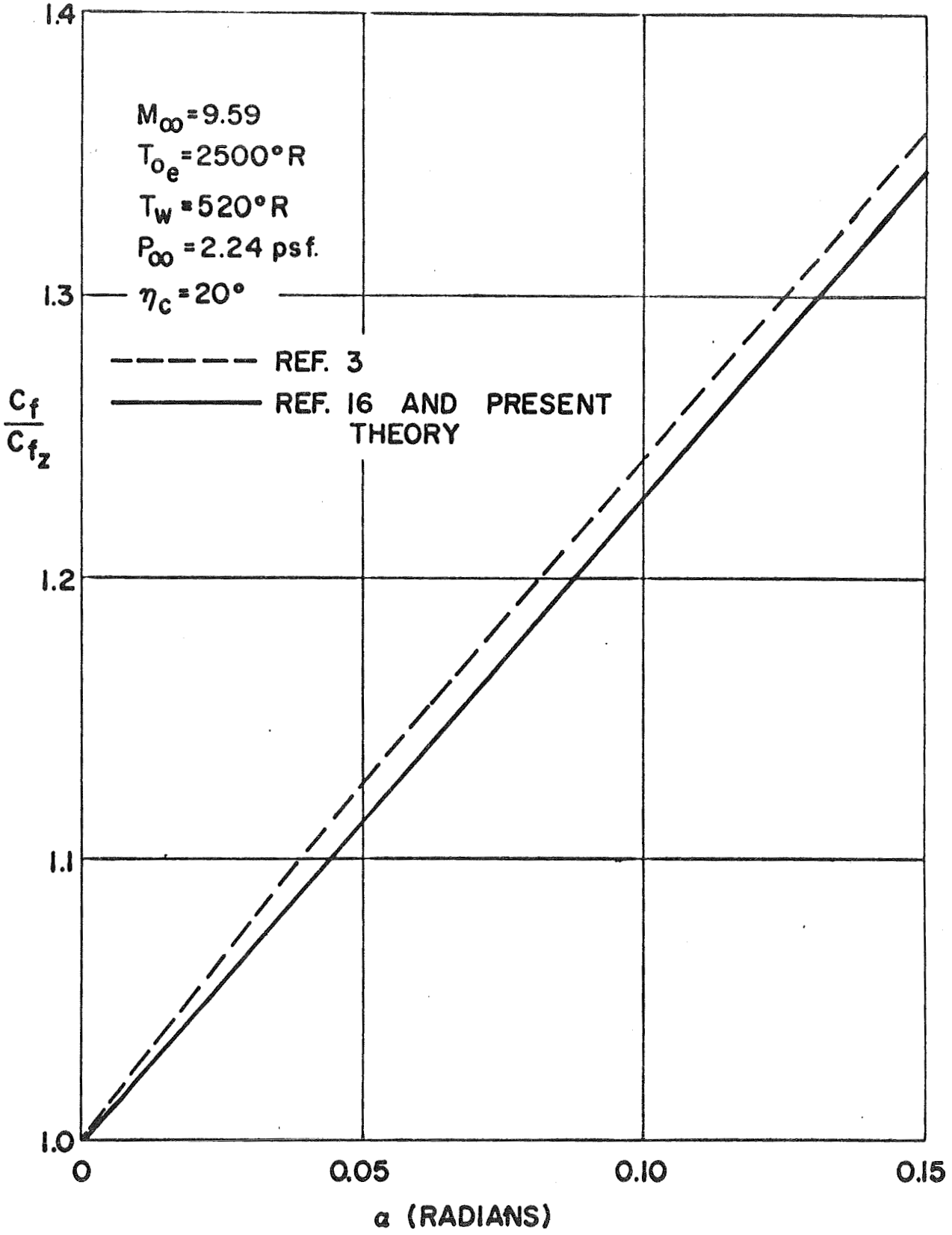


Fig. 5. Coefficient of Friction Variation over Cones and Curved Flares at an Angle of Attack

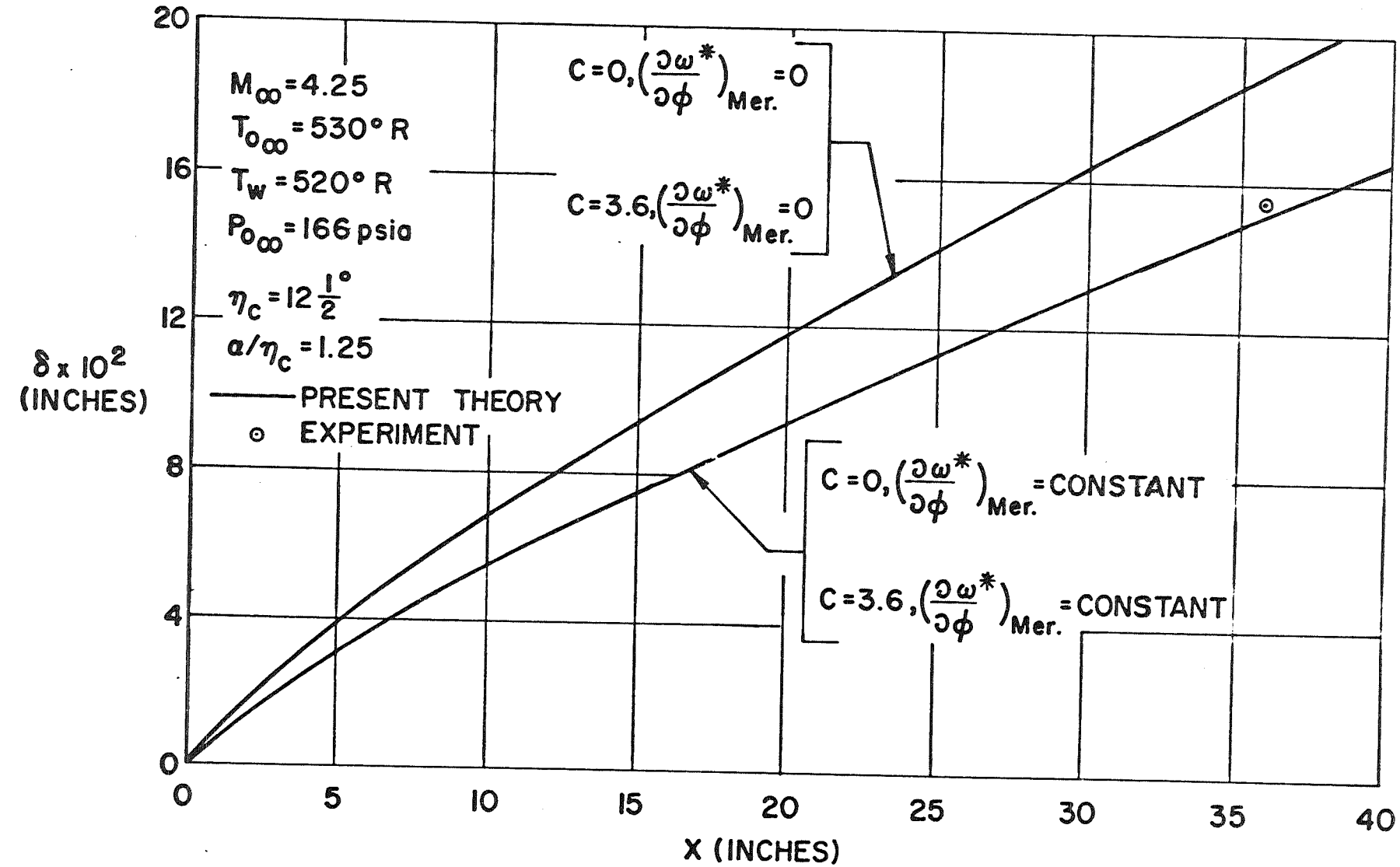


Fig. 6. Boundary Layer Thickness on a Yawed Cone with and without Crossflow

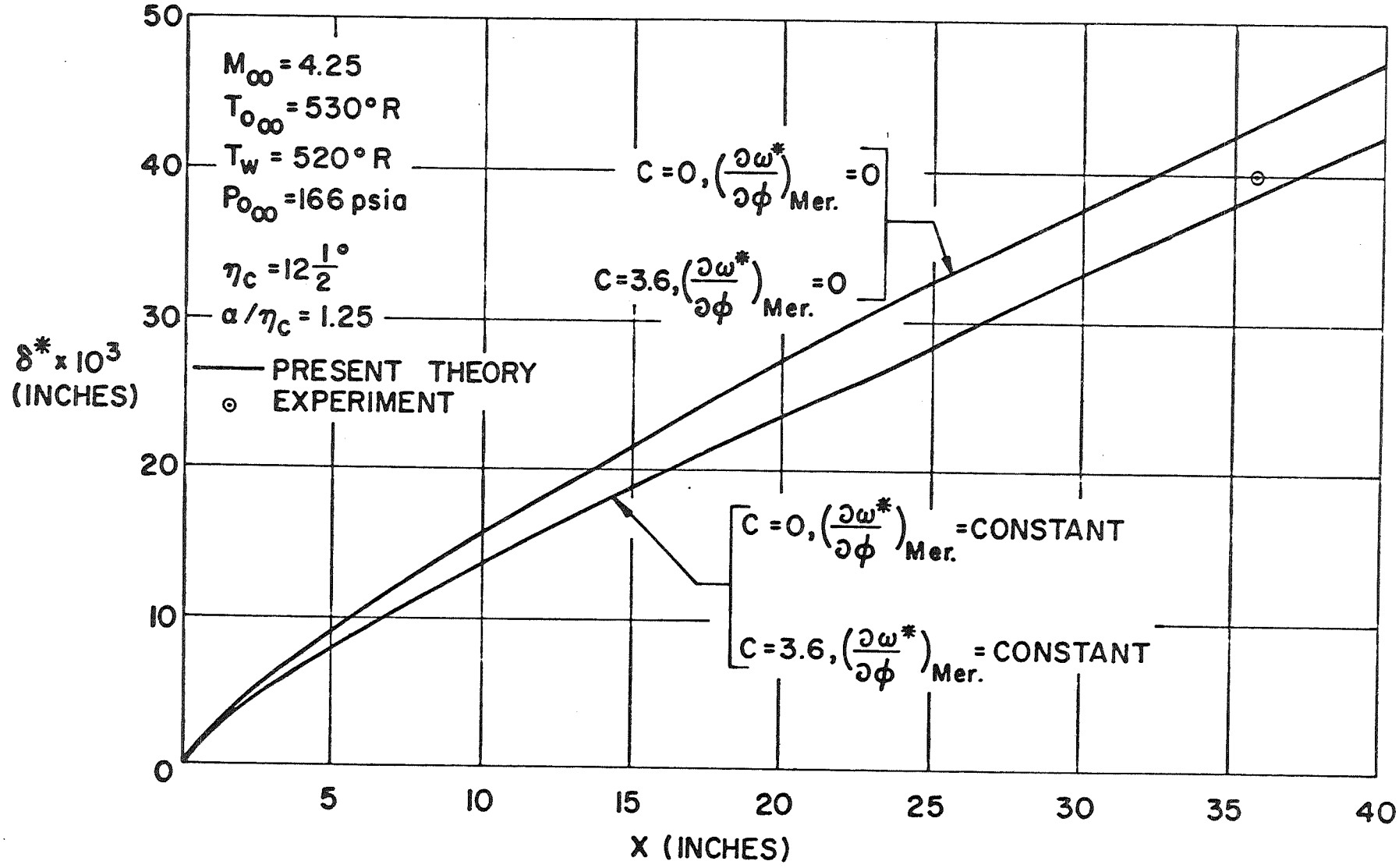


Fig. 7. Displacement Thickness on a Yawed Cone with and without Crossflow

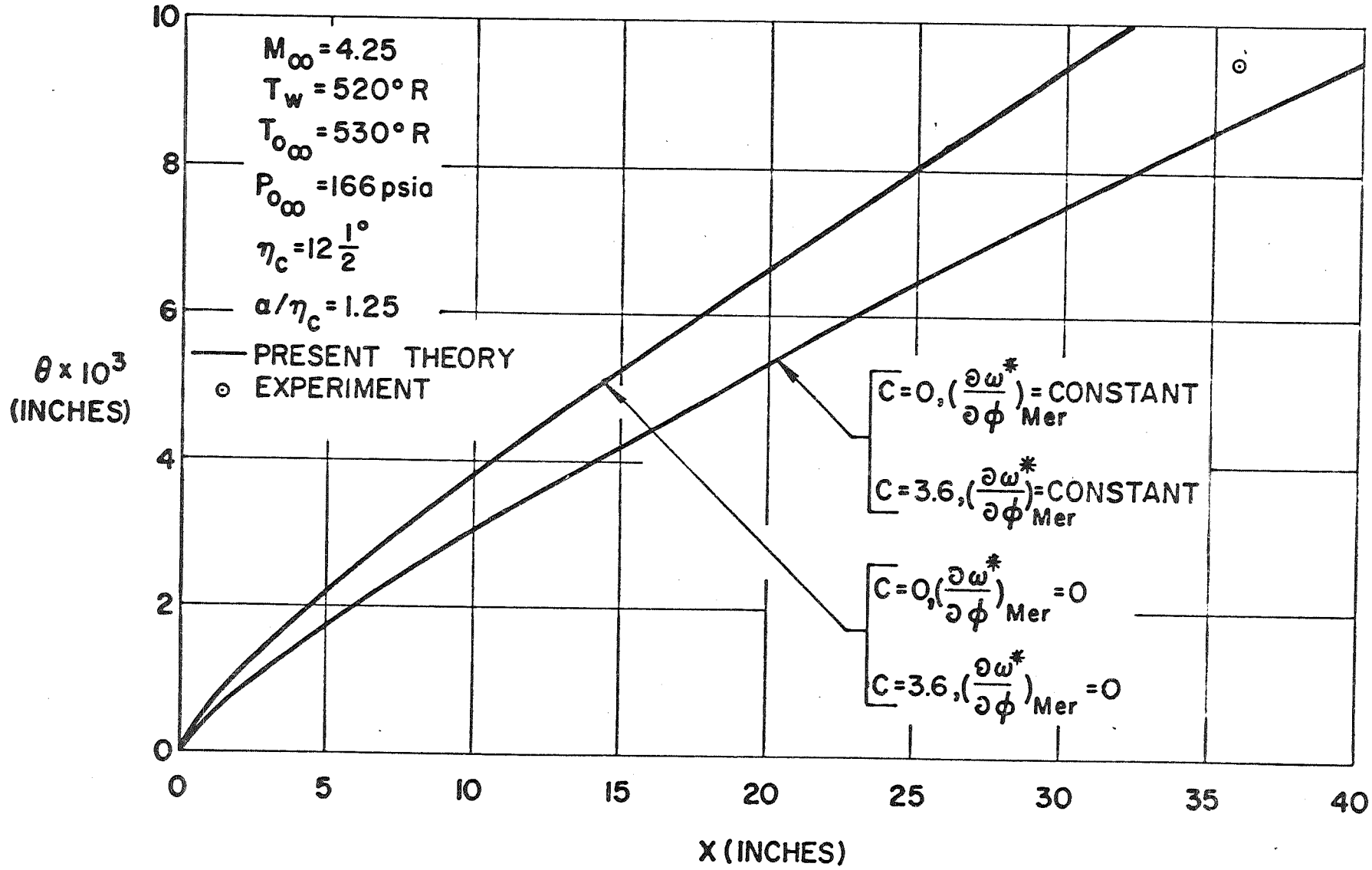


Fig. 8. Momentum Thickness on a Yawed Cone with and without Crossflow

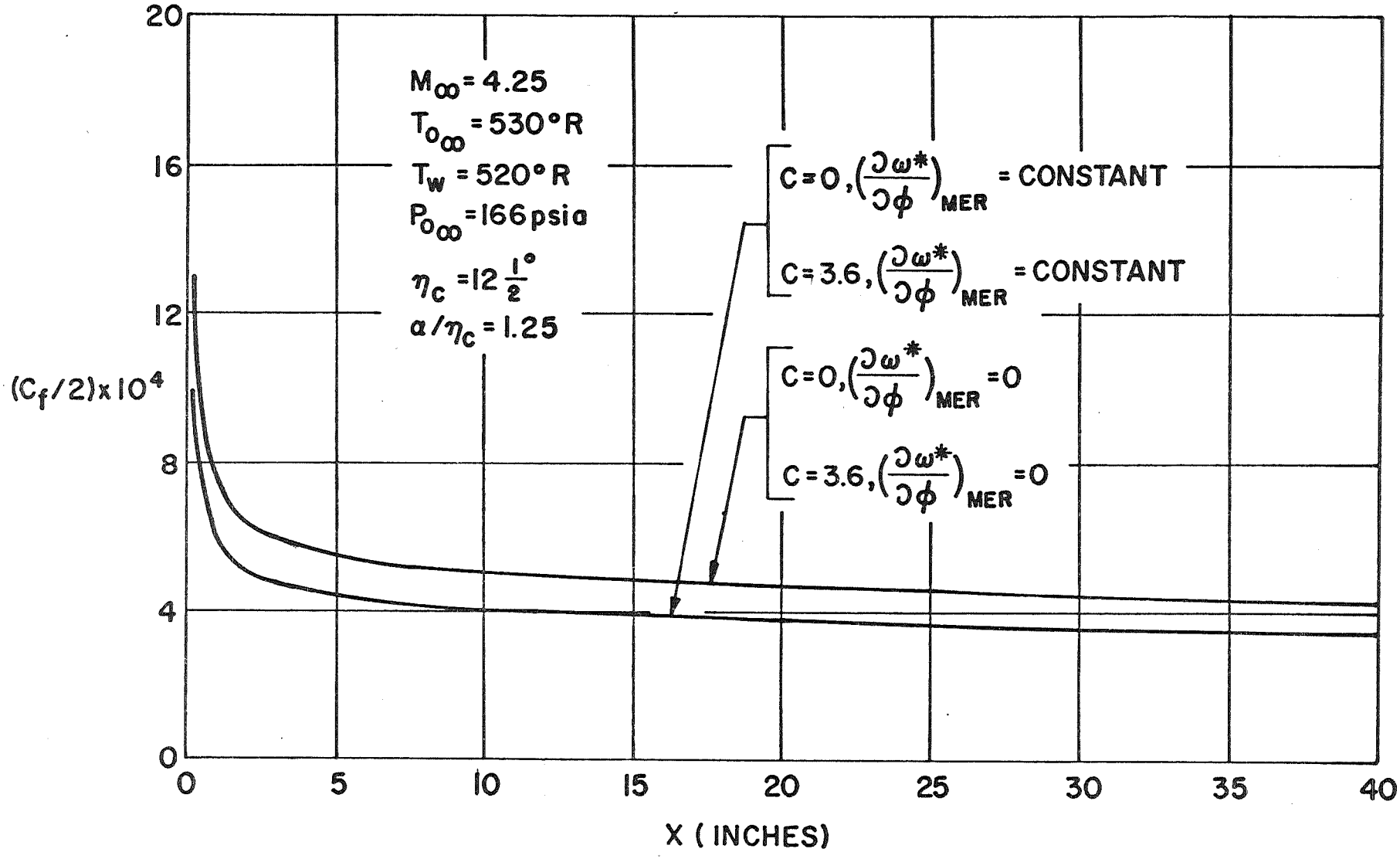


Fig. 9 Coefficient of Friction on a Yawed Cone with and without Crossflow

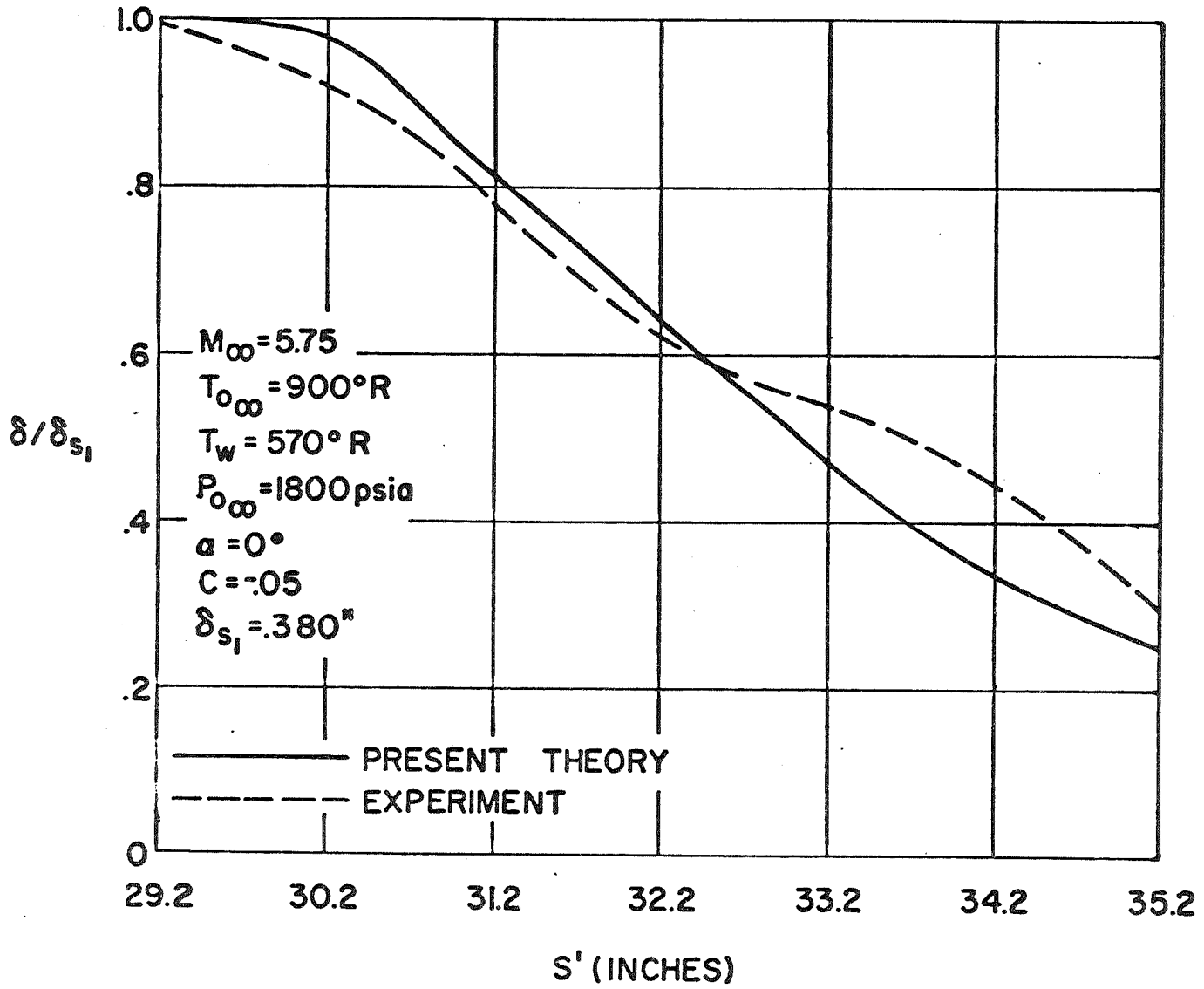


Fig. 10. Boundary Layer Thickness on a Curved Flare in Absence of Crossflow

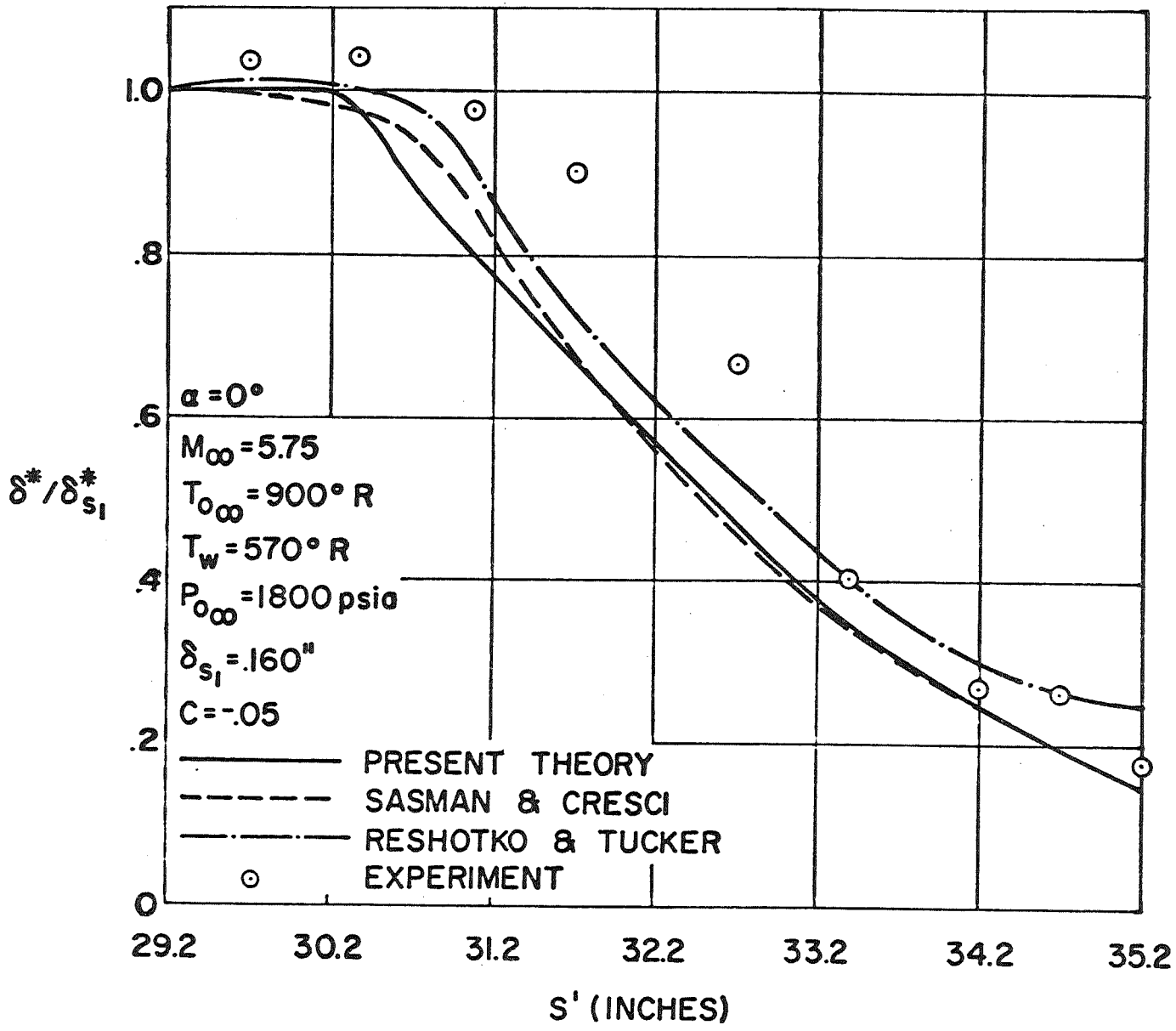


Fig. 11. Displacement Thickness on a Curved Flare in Absence of Crossflow

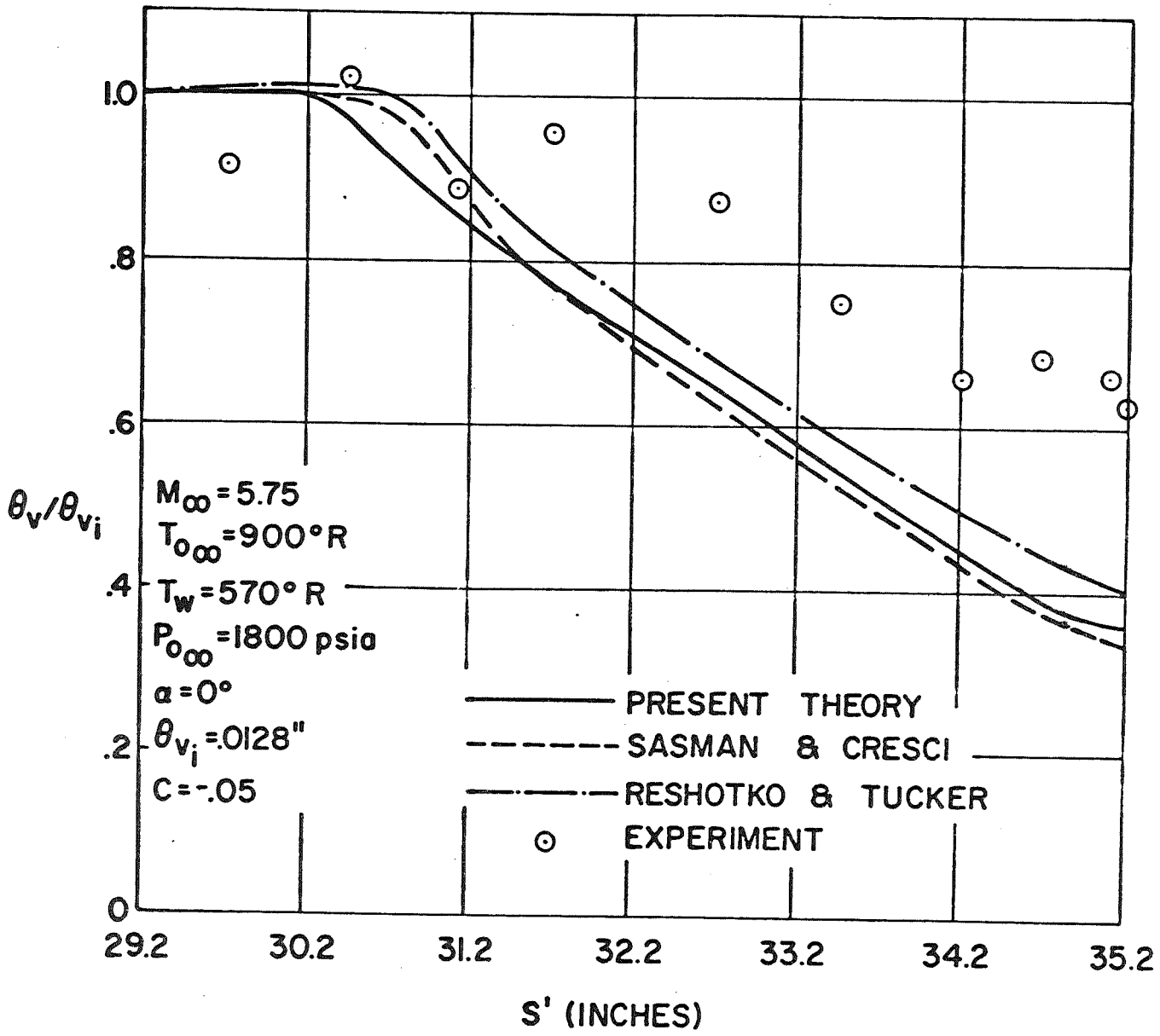


Fig. 12. Momentum Thickness on a Curved Flare in Absence of Cross flow

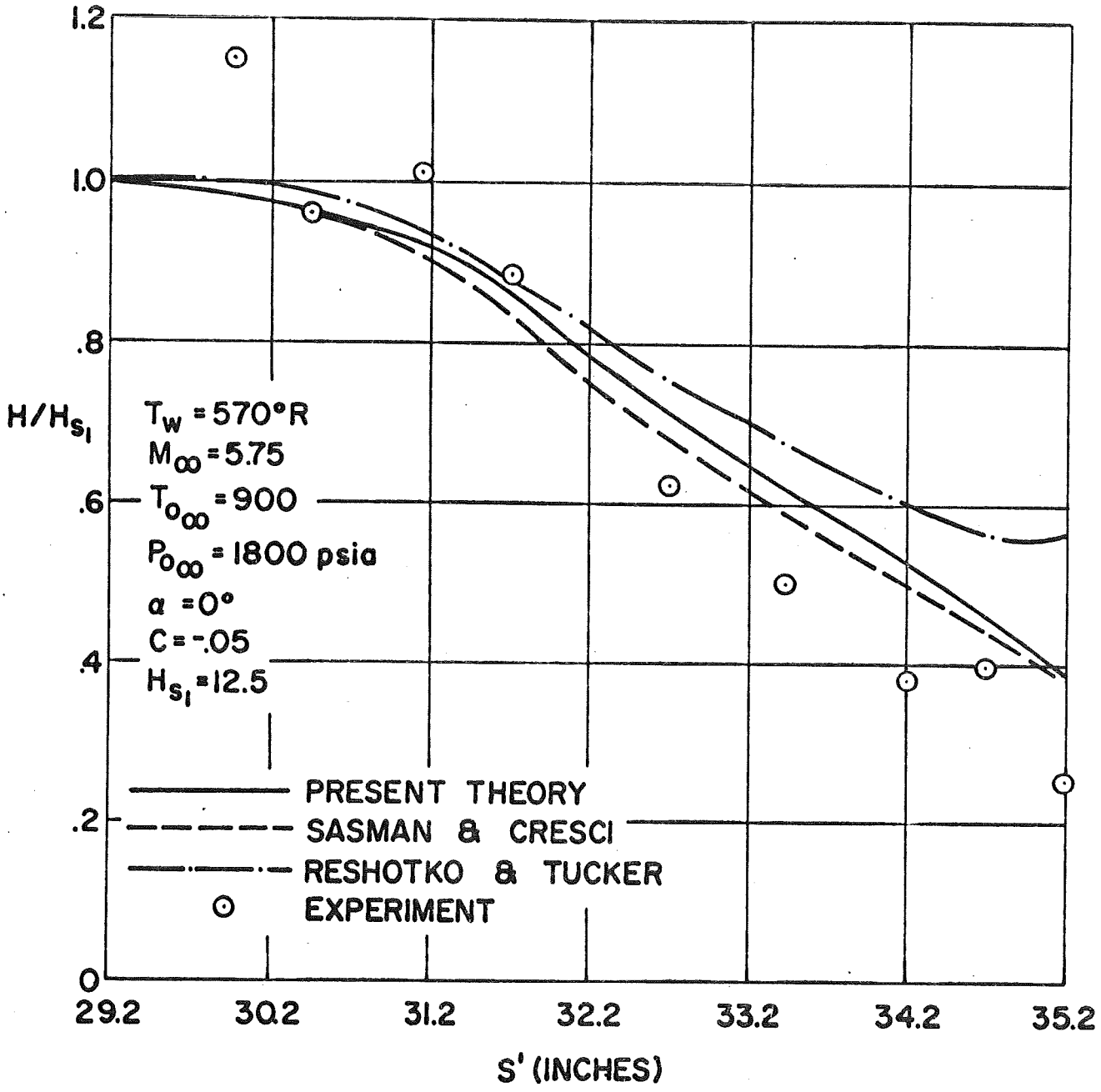


Fig. 13. Form Factor on a Curved Flare in Absence of Crossflow

13. Zakkay & Calarese

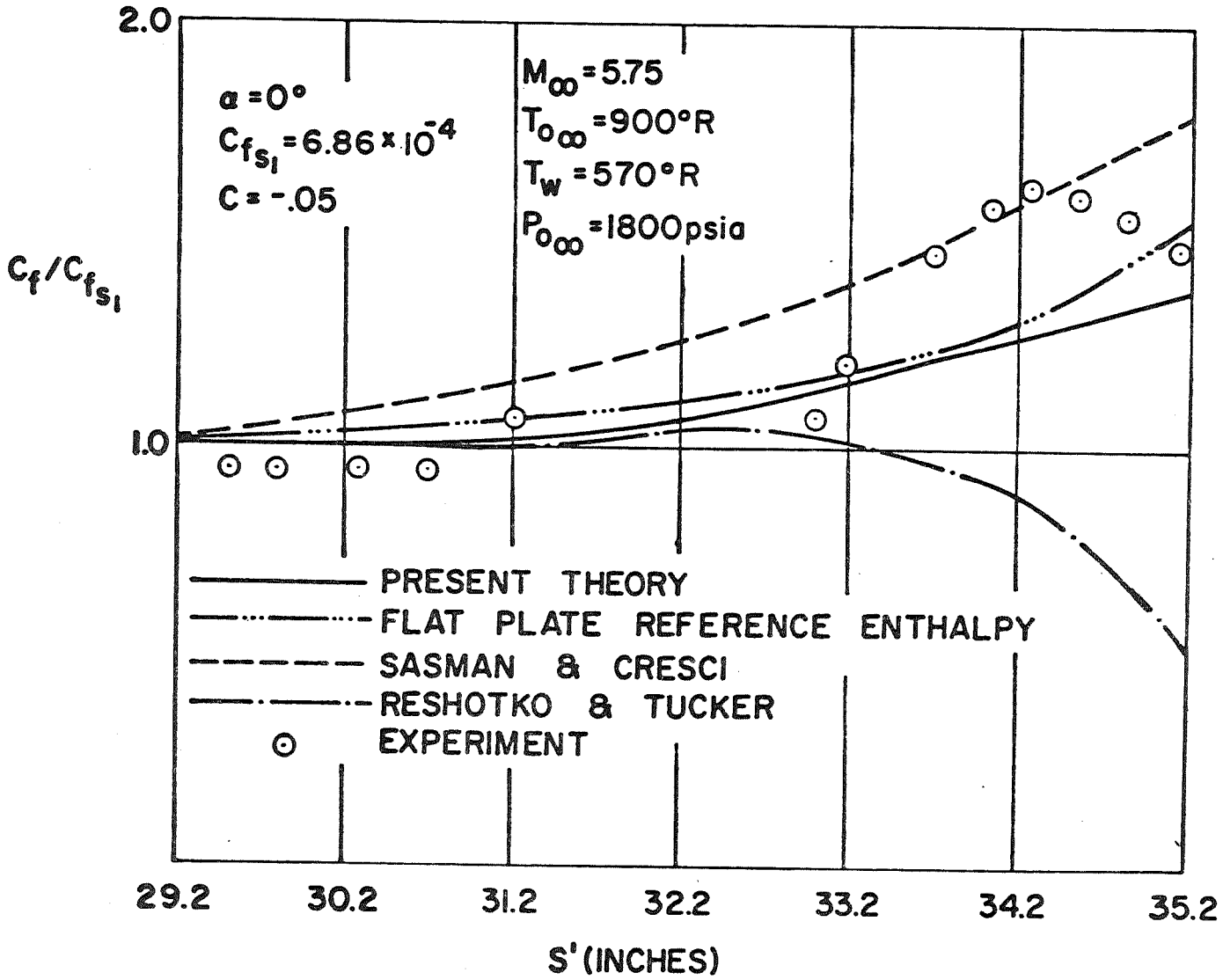


Fig. 14. Coefficient of Friction on a Curved Flare in Absence of Crossflow

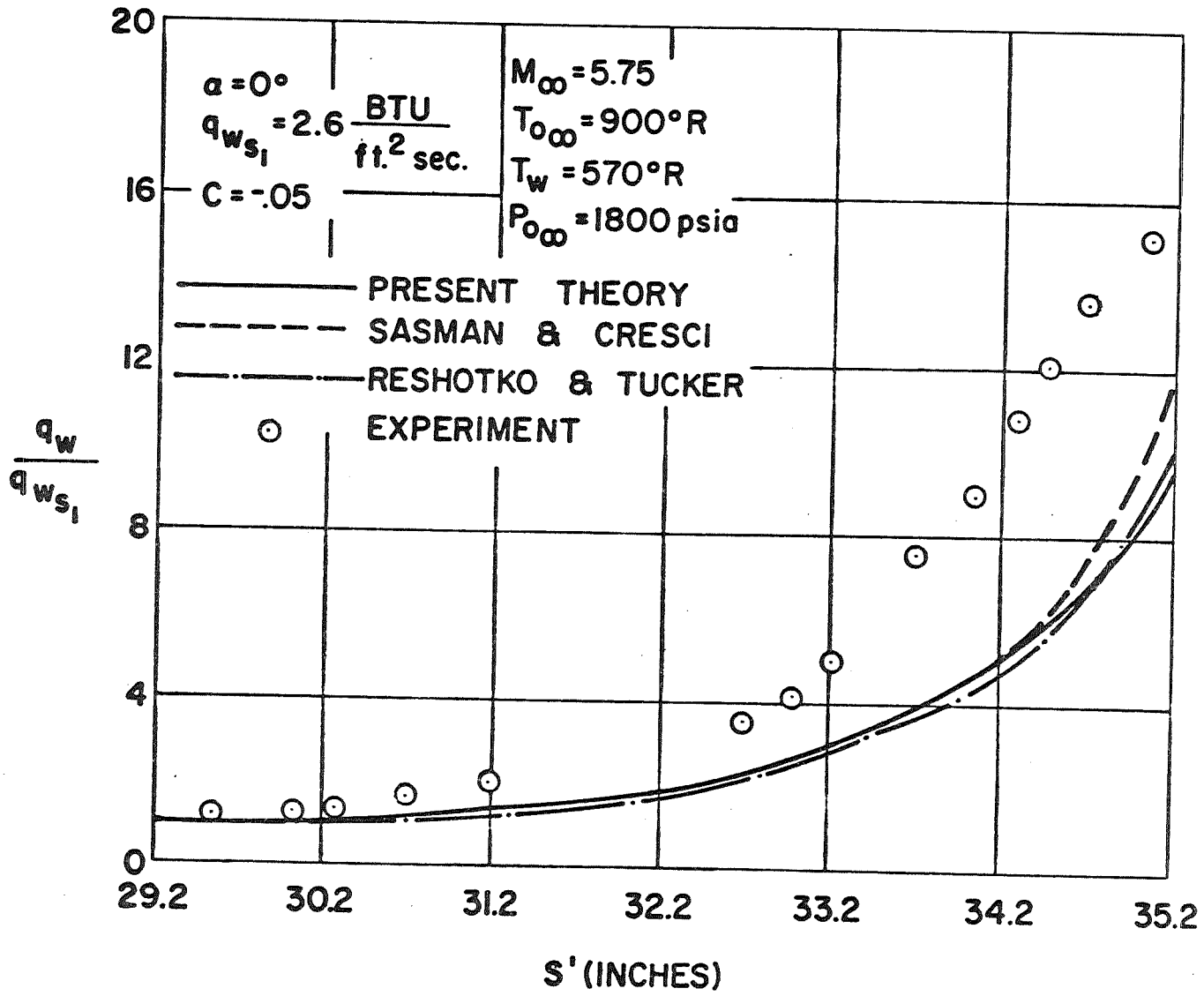


Fig. 15. Heat Transfer on a Curved Flare in Absence of Crossflow

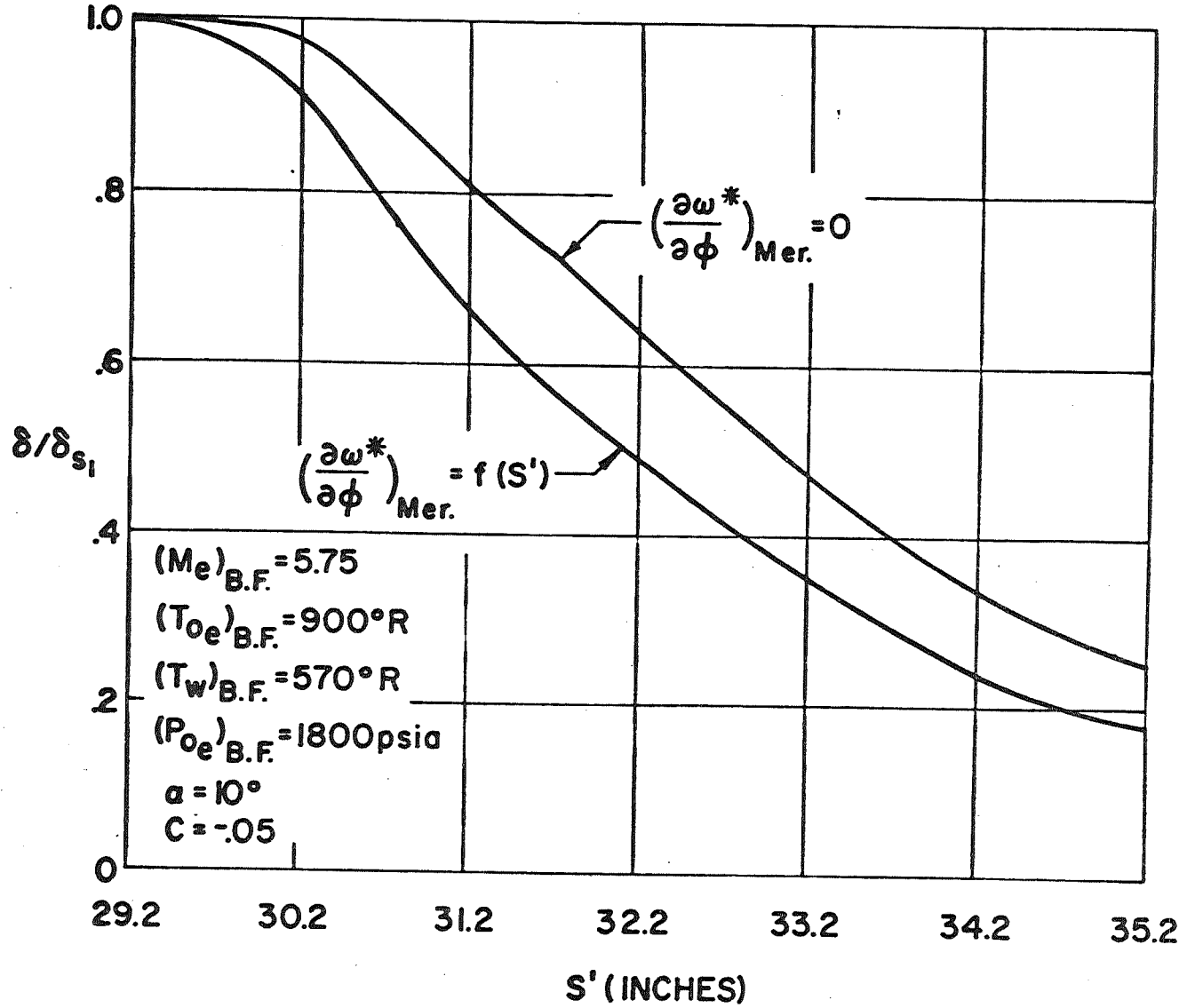


Fig. 16. Boundary Layer Thickness on a Curved Flare with and without Crossflow

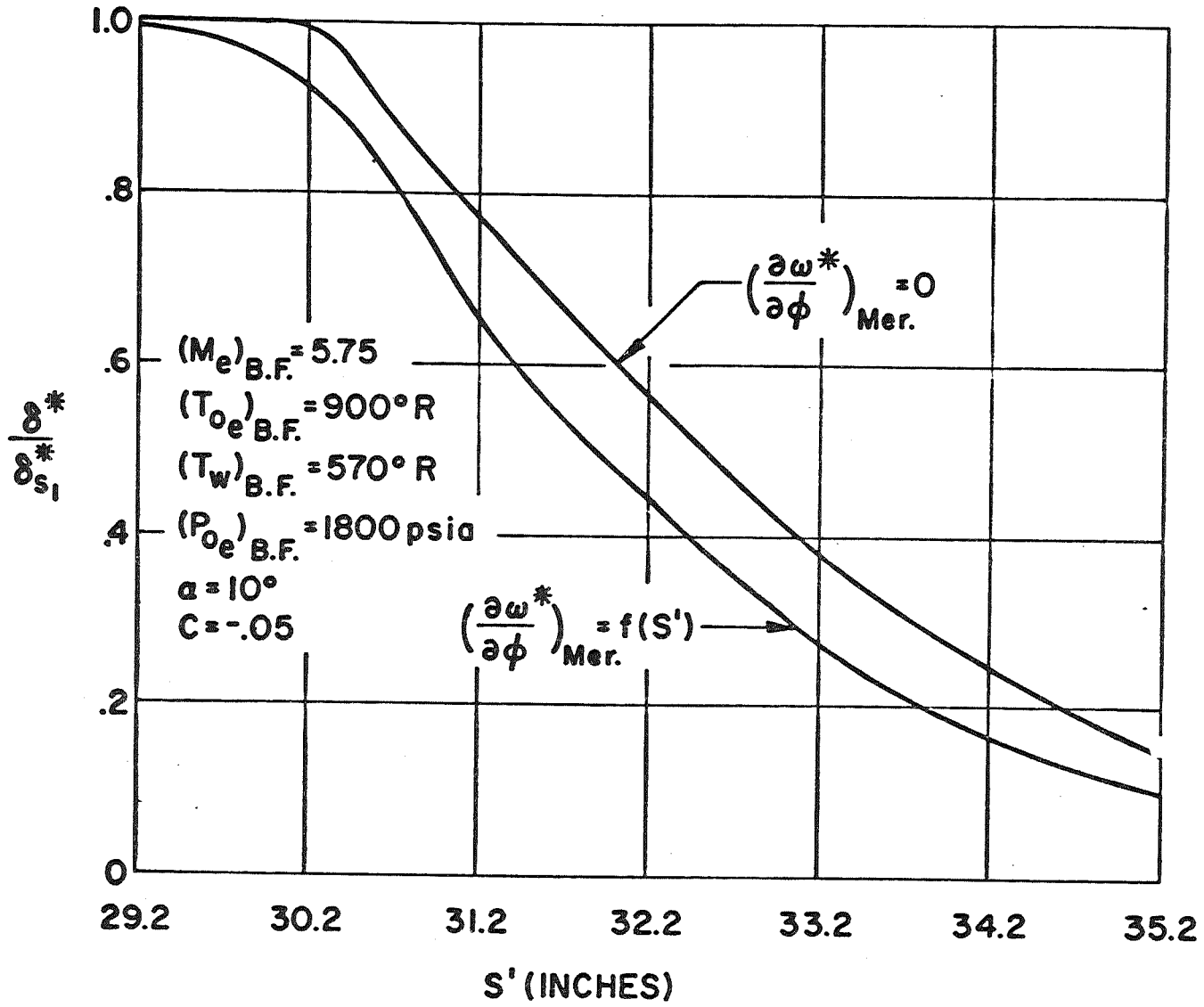


Fig. 17. Displacement Thickness on a Curved Flare with and without Crossflow

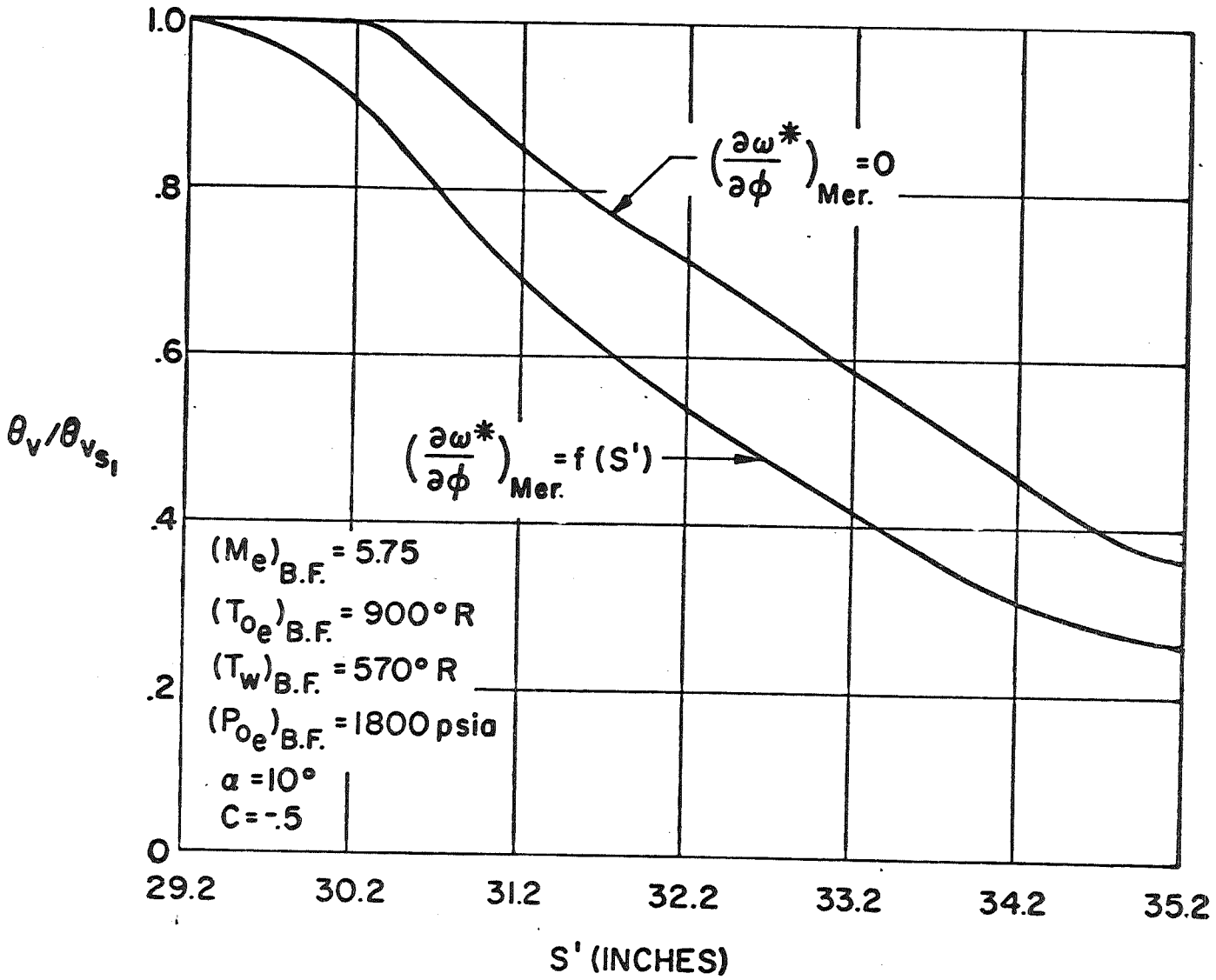


Fig. 18. Momentum Thickness on a Curved Flare with and without Crossflow

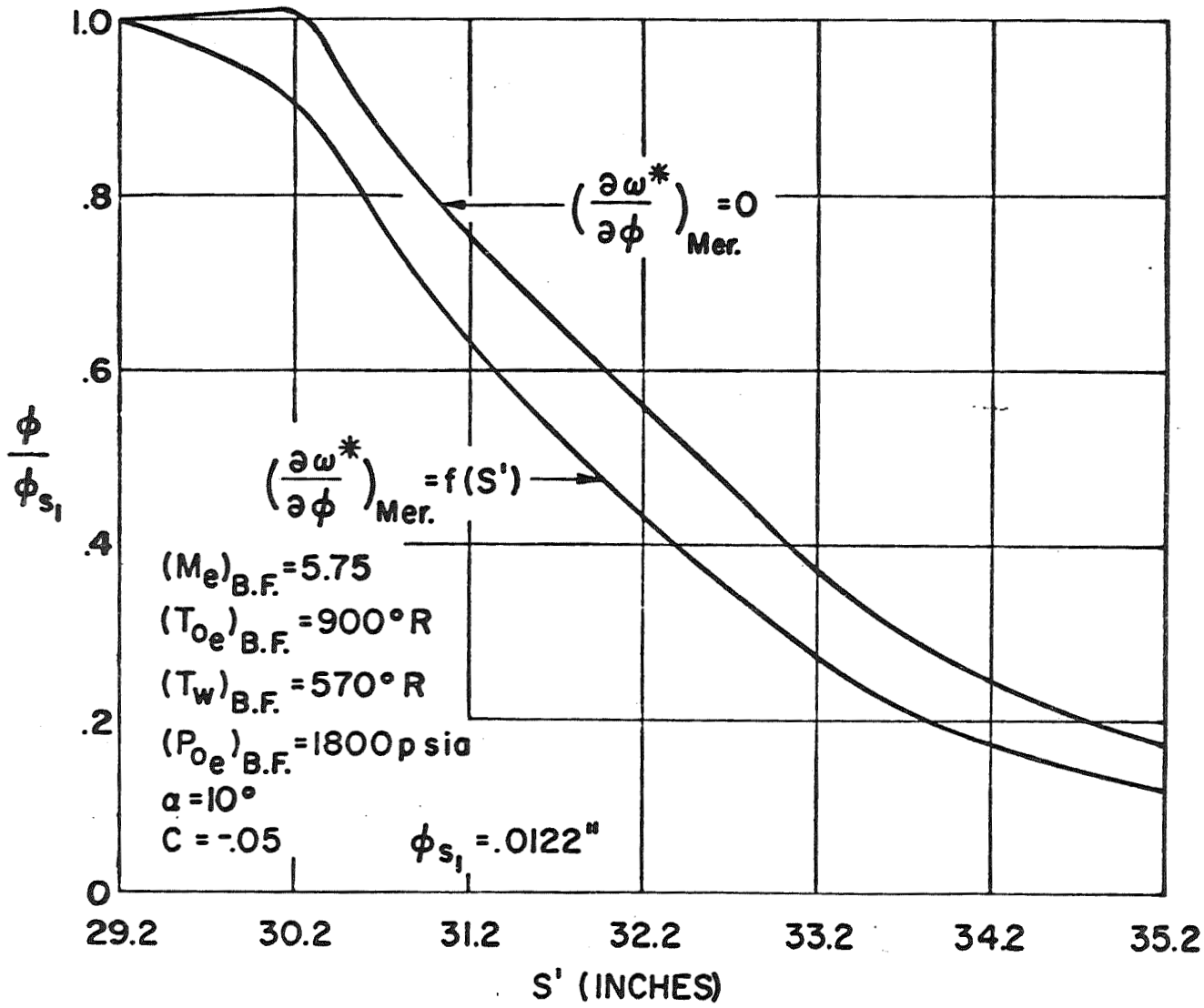


Fig. 19. Energy Thickness on a Curved Flare with and without Crossflow

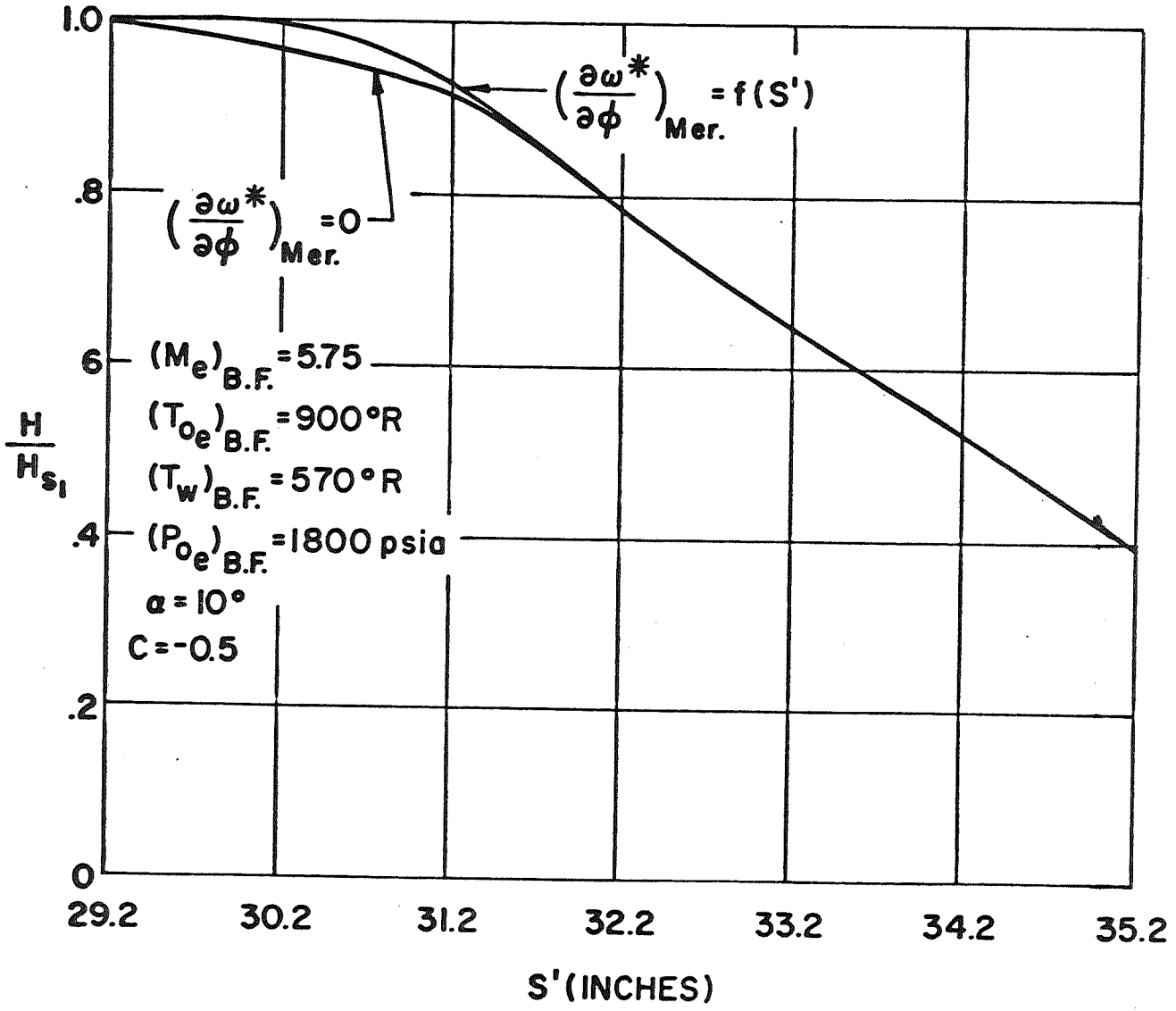


Fig. 20. Form Factor on a Curved Flare with and without Crossflow

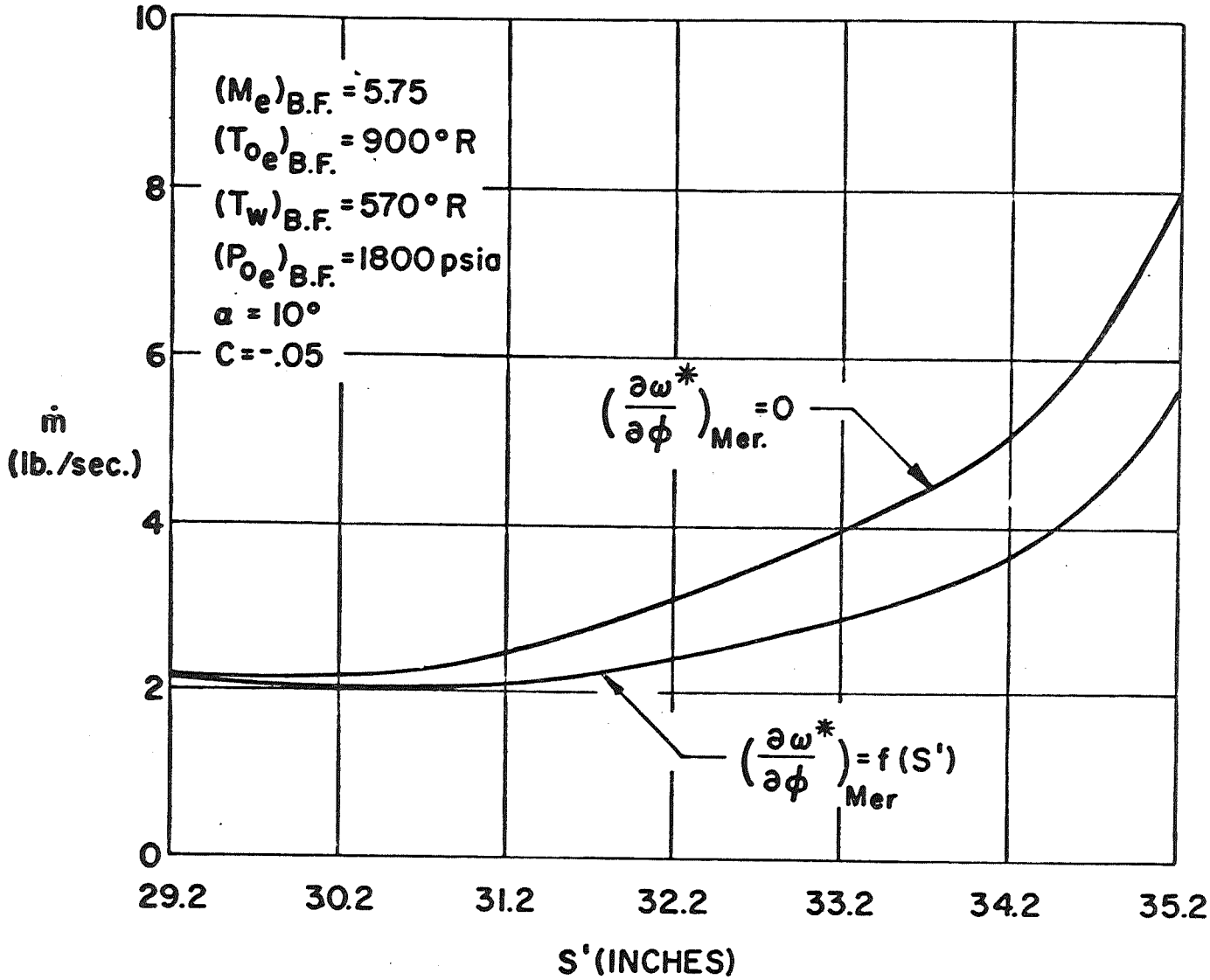


Fig. 21. Mass Flow Over a Compression Flare at an Angle of Attack with and without Crossflow

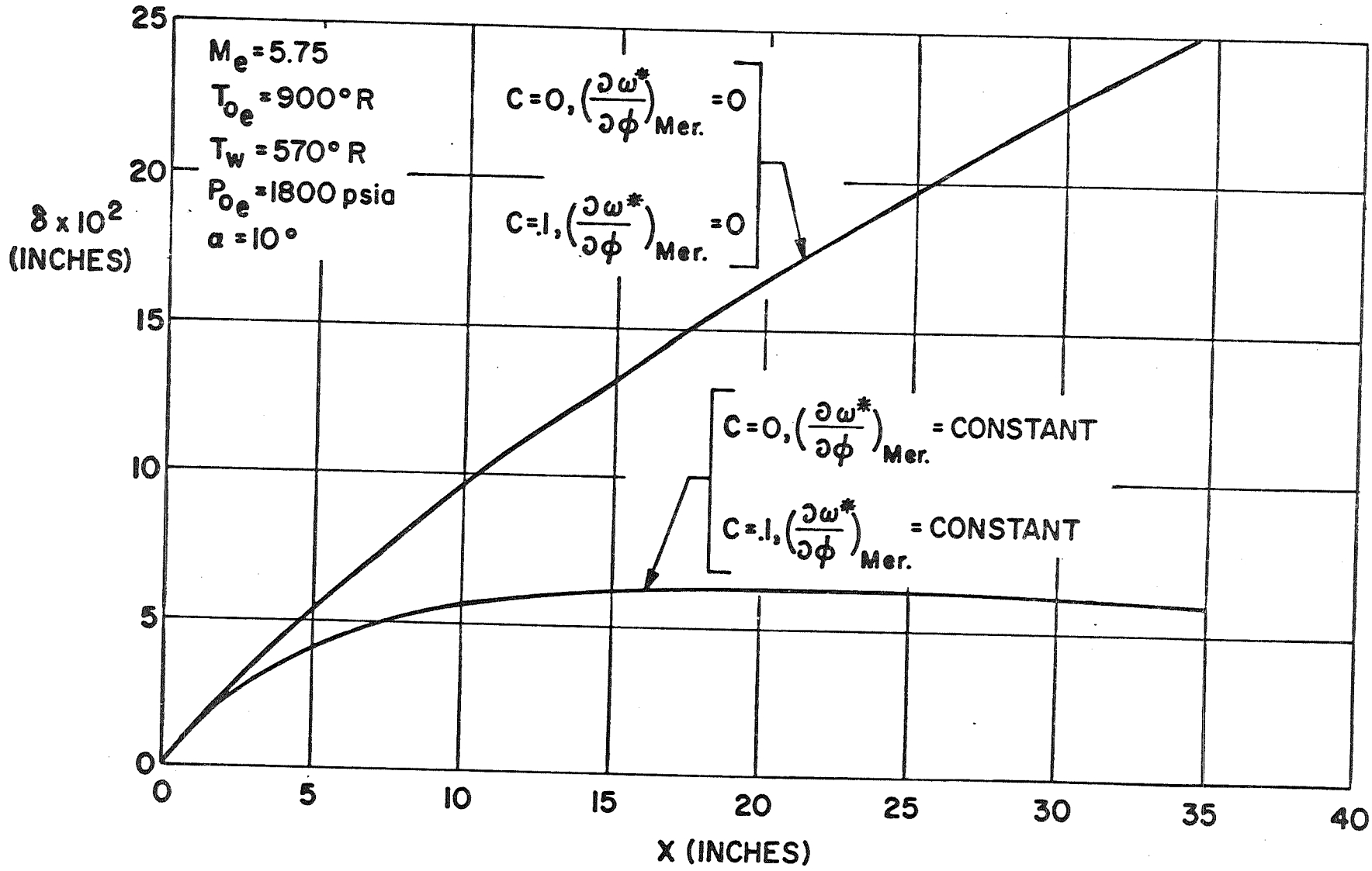


Fig. 22. Boundary Layer Thickness over a Cylinder at an Angle of Attack with and without Crossflow

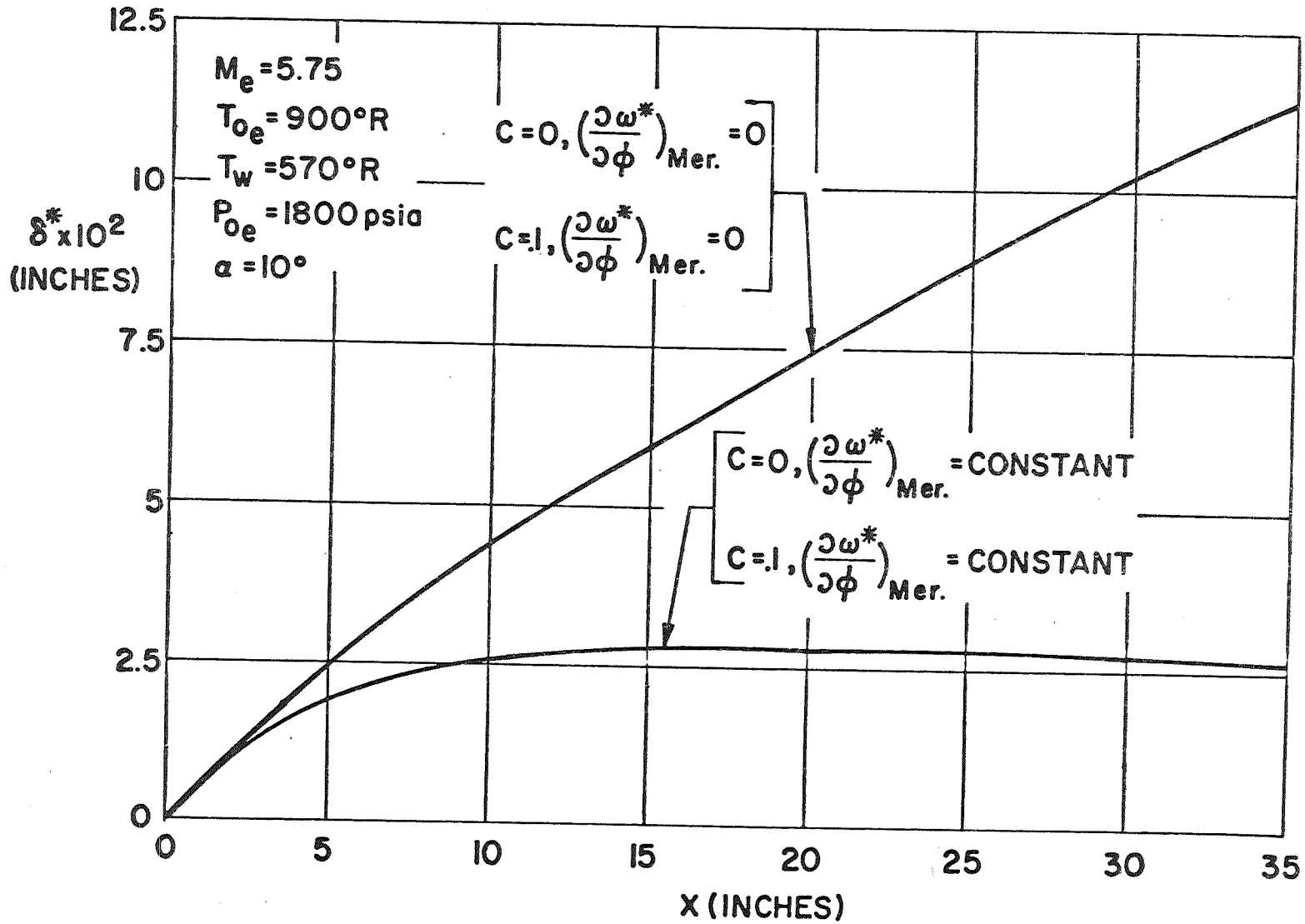


Fig. 23. Displacement Thickness over a Cylinder at an Angle of Attack with and without Crossflow

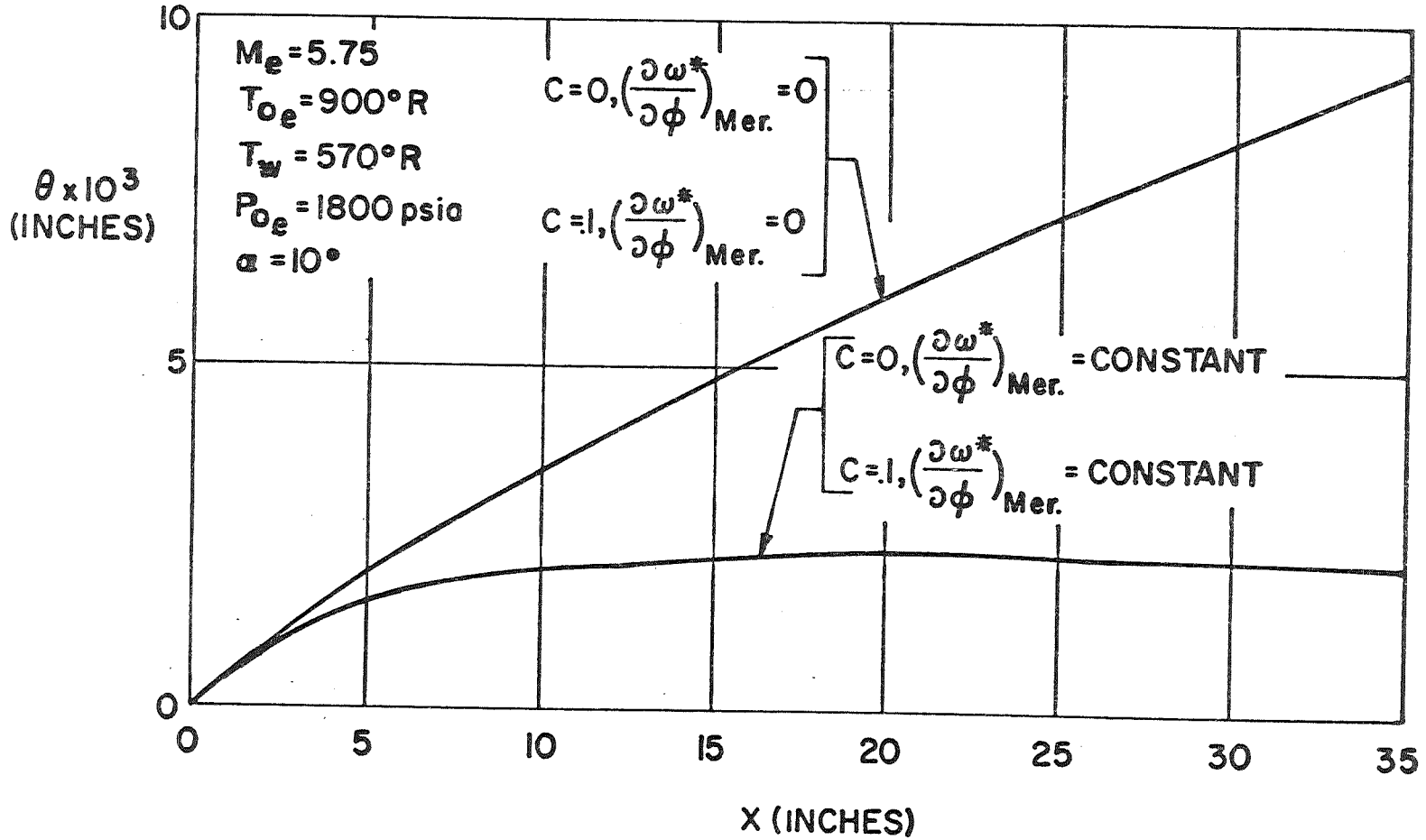


Fig. 24. Momentum Thickness over a Cylinder at an Angle of Attack with and without Crossflow

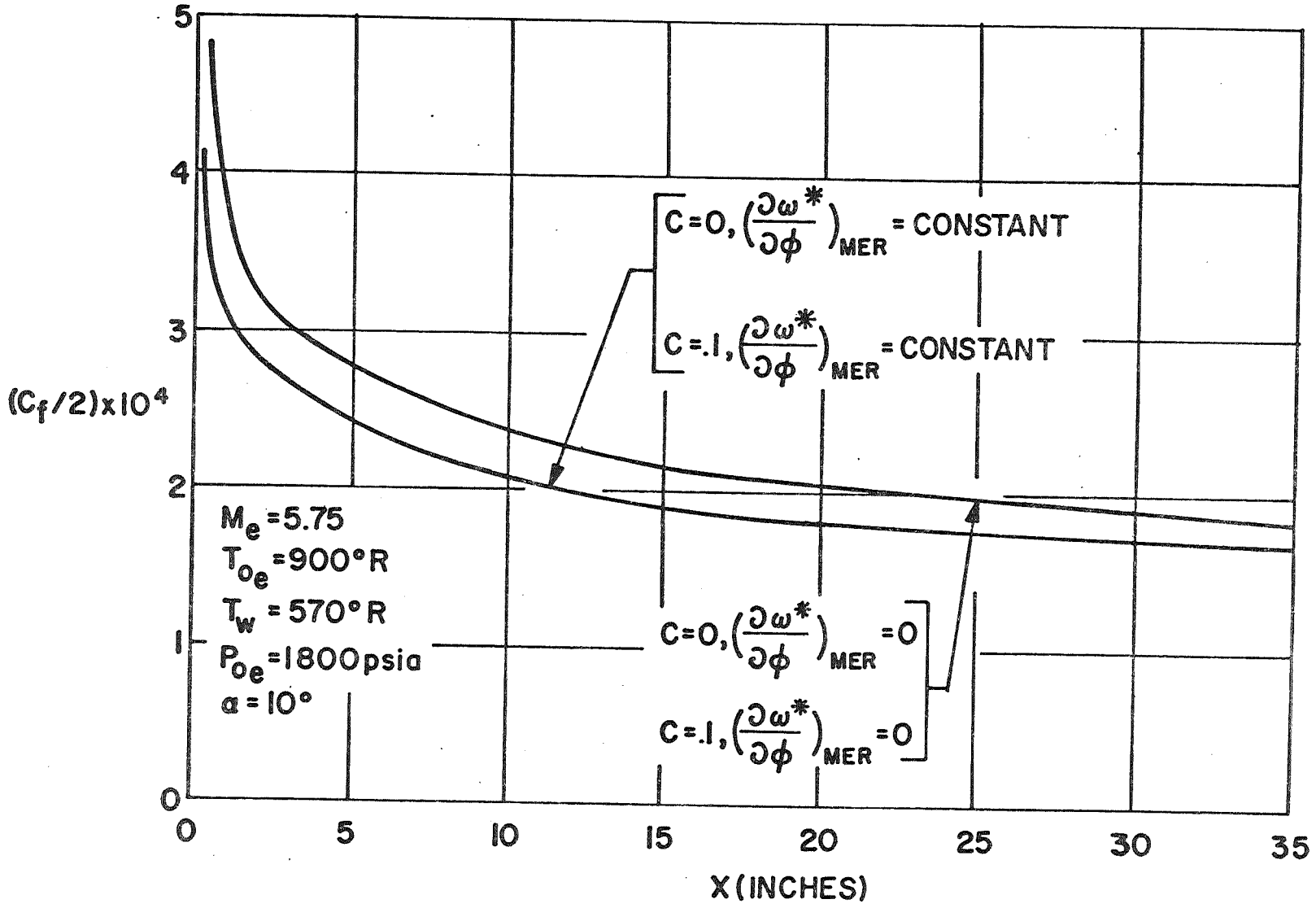


Fig. 25 Coefficient of Friction over a Cylinder at an Angle of Attack with and without Crossflow